

Neutrino Masses and Absence of Flavor Changing Interactions in the 2HDM from Gauge Principles

Miguel D. Campos,^a D. Cogollo,^{b,c} Manfred Lindner,^a T. Melo,^d Farinaldo S. Queiroz,^a Werner Rodejohann^a

^a*Max Planck Institut für Kernphysik, Saupfercheckweg 1, 69117 Heidelberg, Germany*

^b*Departamento de Física, Universidade Federal de Campina Grande, Caixa Postal 10071, 58109-970, Campina Grande, PB, Brazil*

^c*CFTP, Departamento de Física, Instituto Superior Técnico, Universidade de Lisboa*

^d*Departamento de Física, Universidade Federal da Paraíba, João Pessoa, Brazil*

E-mail: farinaldo.queiroz@mpi-hd.mpg.de

ABSTRACT: We propose several Two Higgs Doublet Models with the addition of an Abelian gauge group which free the usual framework from flavor changing neutral interactions and explain neutrino masses through the seesaw mechanism. We discuss the kinetic and mass-mixing gripping phenomenology which encompass several constraints coming from atomic parity violation, the muon anomalous magnetic moment, rare meson decays, Higgs physics, LEP precision data, neutrino-electron scattering, low energy accelerators and LHC probes.

KEYWORDS: flavor problem, 2HDM, neutrinos, $U(1)'$, atomic parity violation, muon magnetic moment, neutrino-electron scattering

Contents

1	Introduction	3
2	The 2HDM Framework	4
3	2HDM with $U(1)_X$ Symmetries	5
3.1	Anomaly Cancellation	6
3.2	Neutrino Masses	8
3.3	Physical Gauge Bosons and Neutral Currents	11
3.4	Z' Decays	13
4	Phenomenological Constraints	16
4.1	Meson Decays	16
4.1.1	Rare K Decays	16
4.1.2	Rare B Decays	17
4.2	Higgs Physics	17
4.2.1	Higgs Properties	17
4.2.2	Higgs Associated Production	18
4.2.3	Higgs Decays	21
4.3	Z Decays	22
4.4	Charged Higgs Searches	23
4.5	Atomic Parity Violation	24
4.6	Muon Anomalous Magnetic Moment	28
4.7	Neutrino-Electron Scattering	29
4.8	Low Energy Accelerators	31
4.9	Discussion	34
5	Conclusions	35
A	Conditions for Anomaly Freedom	36
B	Gauge bosons	37
C	δ Parameter	42
D	Currents for Z and Z'	43
E	Comparison with the 2HDM with Gauged $U(1)_N$	45

1 Introduction

The discovery of a 125 GeV spin-0 scalar announced by the ATLAS [1] and CMS [2] collaborations is a major triumph for the Standard Model (SM). The determination of the scalar sector of particle physics may however not be completed, as there are many extensions of the SM that require additional scalar particles, such as Higgs triplets, singlets or doublets. The ρ parameter provides here a direct constraint on such models, and the value obtained from electroweak precision data of $\rho = 1 \pm 0.0082$ [3] favors for instance small additional vacuum expectation values or scalar doublet representations with hypercharge $0, \pm 1$. In this paper we will study models with an additional Higgs doublet that has identical SM quantum numbers as the usual one. Such Two Higgs Doublet Models (2HDM) are in fact typical in a variety of SM extensions [4].

The 2HDM framework has been proved to be a hospitable environment for axion models [5–7], baryogenesis [8–10], collider physics [11–14], supersymmetry [15], lepton flavor violation [16, 17], and flavor anomalies [18], and a natural environment for new Abelian gauge groups [19–23]. Albeit, the 2HDM framework in its general form is plagued with Flavor Changing Neutral Interactions (FCNI). To cure this FCNI problem, an ad-hoc discrete symmetry is usually evoked. Furthermore, neutrino masses, one of the major observational evidences for new physics, are typically not addressed in 2HDM.

In this work we discuss a gauge solution to the FCNI problem which in addition naturally can incorporate Majorana neutrino masses. The idea is to add a gauged Abelian $U(1)_X$ symmetry to the 2HDM and find anomaly-free models that effectively lead to the usual 2HDM classes that have no FCNI. Anomaly-free models are also possible when right-handed neutrinos are added to the particle content. Their mass terms generate Majorana masses for the light neutrinos. Tracing the absence of dangerous flavor physics and the presence of neutrino masses to the same anomaly-free gauge origin is an attractive approach within 2HDM that deserves careful study. A whole class of models is generated by the idea. A new vector gauge boson that has mass and kinetic-mixing with the SM Z boson is present, and we investigate its phenomenology in a limit which resembles often studied dark photon models. In particular, we address several constraints coming from low energy as well as high energy probes, including atomic parity violation, the muon anomalous magnetic moment, electron-neutrino scattering, and new physics searches at the LHC and several other MeV-GeV colliders such as BaBar.

Our work is structured as follows: In Section 2, we shortly review the 2HDM framework before we augment it in Section 3 with gauged Abelian symmetries and

study the constraints on the models from anomaly cancellation, including right-handed neutrinos. In Section 4 the models are confronted with various phenomenological constraints before we conclude in Section 5. Some details are delegated to appendices.

2 The 2HDM Framework

In the Standard Model, one scalar doublet accounts for the masses of all charged fermions and gauge bosons. However, extended scalar sectors are also possible. Among the various constraints on such cases, the ρ parameter is particularly well constrained by electroweak precision data [24]; it is defined as,

$$\rho = \frac{\sum_{i=1}^n [I_i (I_i + 1) - \frac{1}{4} Y_i^2] v_i}{\sum_{i=1}^n \frac{1}{2} Y_i^2 v_i}. \quad (2.1)$$

Here I_i and Y_i are the isospin and hypercharge of a scalar representation with vev v_i . The value $\rho = 1$ is not altered by the addition of scalar doublets under $SU(2)$ with hypercharge $Y = \pm 1$, or scalar singlets with $Y = 0$. Therefore, enlarging the Standard Model with a scalar doublet under $SU(2)$ is a natural and popular framework, the so-called the Two Higgs Doublet Model (2HDM) [25].

In the 2HDM the most general potential for two doublets with hypercharge $Y = 1$, gauge invariant and renormalizable, is given by,

$$\begin{aligned} V(\Phi_1, \Phi_2) = & m_{11}^2 \Phi_1^\dagger \Phi_1 + m_{22}^2 \Phi_2^\dagger \Phi_2 - \left(m_{12}^2 \Phi_1^\dagger \Phi_2 + h.c. \right) + \frac{\lambda_1}{2} \left(\Phi_1^\dagger \Phi_1 \right)^2 \\ & + \frac{\lambda_2}{2} \left(\Phi_2^\dagger \Phi_2 \right)^2 + \lambda_3 \left(\Phi_1^\dagger \Phi_1 \right) \left(\Phi_2^\dagger \Phi_2 \right) + \lambda_4 \left(\Phi_1^\dagger \Phi_2 \right) \left(\Phi_2^\dagger \Phi_1 \right) \\ & + \left[\frac{\lambda_5}{2} \left(\Phi_1^\dagger \Phi_2 \right)^2 + \lambda_6 \left(\Phi_1^\dagger \Phi_1 \right) \left(\Phi_1^\dagger \Phi_2 \right) + \lambda_7 \left(\Phi_2^\dagger \Phi_2 \right) \left(\Phi_1^\dagger \Phi_2 \right) + h.c. \right]. \end{aligned} \quad (2.2)$$

The Yukawa Lagrangian reads

$$\begin{aligned} -\mathcal{L}_{Y_{2\text{HDM}}} = & y^{1d} \bar{Q}_L \Phi_1 d_R + y^{1u} \bar{Q}_L \tilde{\Phi}_1 u_R + y^{1e} \bar{L}_L \Phi_1 e_R \\ & + y^{2d} \bar{Q}_L \Phi_2 d_R + y^{2u} \bar{Q}_L \tilde{\Phi}_2 u_R + y^{2e} \bar{L}_L \Phi_2 e_R + h.c., \end{aligned} \quad (2.3)$$

where

$$\Phi_i = \begin{pmatrix} \phi_i^+ \\ (v_i + \rho_i + i\eta_i) / \sqrt{2} \end{pmatrix}. \quad (2.4)$$

Having two Higgs doublets generating masses for all fermions leads in general to the presence of FCNI at tree level, subjecting the model to tight bounds from flavor probes [26]. The easy solution [27, 28] to this issue is the evocation of an ad-hoc Z_2 symmetry, where in particular,

$$\Phi_1 \rightarrow -\Phi_1, \quad \Phi_2 \rightarrow +\Phi_2, \quad (2.5)$$

also known as the Natural Flavor Conservation (NFC) criterion.

Assuming CP conservation, the transformations in Eq. (2.5) yield a new scalar potential,

$$\begin{aligned} V(\Phi_1, \Phi_2) = & m_{11}^2 \Phi_1^\dagger \Phi_1 + m_{22}^2 \Phi_2^\dagger \Phi_2 - m_{12}^2 \left(\Phi_1^\dagger \Phi_2 + \Phi_2^\dagger \Phi_1 \right) + \frac{\lambda_1}{2} \left(\Phi_1^\dagger \Phi_1 \right)^2 \\ & + \frac{\lambda_2}{2} \left(\Phi_2^\dagger \Phi_2 \right)^2 + \lambda_3 \left(\Phi_1^\dagger \Phi_1 \right) \left(\Phi_2^\dagger \Phi_2 \right) + \lambda_4 \left(\Phi_1^\dagger \Phi_2 \right) \left(\Phi_2^\dagger \Phi_1 \right) \\ & + \frac{\lambda_5}{2} \left[\left(\Phi_1^\dagger \Phi_2 \right)^2 + \left(\Phi_2^\dagger \Phi_1 \right)^2 \right]. \end{aligned} \quad (2.6)$$

Here the m_{12} term softly violates the condition in Eq. (2.5), in order to avoid domain walls. The discrete symmetry Eq. (2.5) will eliminate some of the terms in the general Yukawa Lagrangian Eq. (2.3) avoiding also the FCNI. Which terms will be eliminated depends upon the parity assignment of the fermions under Z_2 . We can, for example, consider that all fermions are even under Z_2 transformation. In this case $\mathcal{L}_{Y_{2\text{HDM}}}$ becomes,

$$-\mathcal{L}_{Y_{2\text{HDM}}} = y_2^d \bar{Q}_L \Phi_2 d_R + y_2^u \bar{Q}_L \tilde{\Phi}_2 u_R + y_2^e \bar{L}_L \Phi_2 e_R + h.c., \quad (2.7)$$

with only Φ_2 coupling to fermions. This is the Type I 2HDM. Other choices of fermion parities are presented in Table 1; the four 2HDM shown in the table are subject to different phenomenologies and constraints (see [4] for a review).

After this short summary of the general 2HDM framework, we will discuss how to base those flavor-safe models on a gauged $U(1)_X$.

3 2HDM with $U(1)_X$ Symmetries

A fundamental solution to the flavor problem in the 2HDM could come from well-established gauge principles. It is known that an Abelian gauge symmetry when spontaneously broken gives rise to a discrete symmetry, simply because the latter is a subgroup of the former. The quantum numbers of the particles charged under the new $U(1)_X$ symmetry will dictate what is the remnant symmetry. It has been shown that the necessary Z_2 symmetry to cure 2HDM from FCNI can be generated from gauge principles [29] under certain conditions. In what follows we will review these conditions using general arguments and address the implications.

Model	Φ_1	Φ_2	u_R	d_R	e_R	Q_L	L_L
Type I	–	+	+	+	+	+	+
Type II	–	+	+	–	–	+	+
Lepton-specific	–	+	+	+	–	+	+
Flipped	–	+	+	–	+	+	+

Table 1: Different types of 2HDM according to the Z_2 parities of the SM fermions. In the type I only Φ_2 couples to all SM fermions; In the type II Φ_2 couples to up quarks and Φ_1 couples to leptons and down quarks. In the third type of 2HDM, also known as lepton-specific, Φ_1 couples to leptons while Φ_2 couples to quarks. Lastly, in the fourth type, called flipped 2HDM, the scalar doublet Φ_1 couples to down quarks while Φ_2 couples to leptons and up quarks.

3.1 Anomaly Cancellation

In order to truly prevent FCNI in the 2HDM, and mimic the effect of the Z_2 symmetry at lower energies, the scalar doublets Φ_1 and Φ_2 have to transform differently under $U(1)_X$, reducing the scalar potential to

$$\begin{aligned}
V(\Phi_1, \Phi_2) = & m_{11}^2 \Phi_1^\dagger \Phi_1 + m_{22}^2 \Phi_2^\dagger \Phi_2 + \frac{\lambda_1}{2} (\Phi_1^\dagger \Phi_1)^2 + \frac{\lambda_2}{2} (\Phi_2^\dagger \Phi_2)^2 \\
& + \lambda_3 (\Phi_1^\dagger \Phi_1) (\Phi_2^\dagger \Phi_2) + \lambda_4 (\Phi_1^\dagger \Phi_2) (\Phi_2^\dagger \Phi_1).
\end{aligned} \tag{3.1}$$

In addition, one needs to successfully generate fermion masses by properly choosing the transformations of the fermions under the $U(1)_X$ symmetry. The requirement that the scalar doublets transform differently still leaves enough freedom to construct several models, based on the specific charge assignments for the Standard Model particles. We shall see what kind models one can build using simply gauge invariance and anomaly cancellation.

Generally speaking, a local transformation shifts the fields as follows,

$$\begin{aligned}
L_L & \rightarrow L'_L = e^{il\alpha(x)} L_L \\
Q_L & \rightarrow Q'_L = e^{iq\alpha(x)} Q_L \\
e_R & \rightarrow e'_R = e^{ie\alpha(x)} e_R \\
u_R & \rightarrow u'_R = e^{iu\alpha(x)} u_R \\
d_R & \rightarrow d'_R = e^{id\alpha(x)} d_R \\
\Phi_1 & \rightarrow \Phi'_1 = e^{ih_1\alpha(x)} \Phi_1 \\
\Phi_2 & \rightarrow \Phi'_2 = e^{ih_2\alpha(x)} \Phi_2,
\end{aligned} \tag{3.2}$$

where l, q, e, u, d, h_1, h_2 are the charges of the fields under $U(1)_X$. Once we write down a Yukawa Lagrangian and demand gauge invariance, the transformations in Eq. (3.2) are no longer arbitrary, and the charges under $U(1)_X$ will be interconnected. In the

Type I 2HDM, on which we focus in this paper, where fermions couple only with Φ_2 , see Eq. (2.7), the following $U(1)_X$ transformations apply:

$$\begin{aligned}
-\mathcal{L}_{Y_{2\text{HDM}}} \rightarrow -\mathcal{L}'_{Y_{2\text{HDM}}} &= e^{(-q+h_2+d)i\alpha} y_2^d \bar{Q}_L \Phi_2 d_R + e^{(-q-h_2+u)i\alpha} y_2^u \bar{Q}_L \tilde{\Phi}_2 u_R \\
&+ e^{(-l+h_2+e)i\alpha} y_2^e \bar{L}_L \Phi_2 e_R + h.c.
\end{aligned} \tag{3.3}$$

The $U(1)_X$ invariance imposes the following conditions on the charges of the fields:

$$\begin{aligned}
d - q + h_2 &= 0 \\
u - q - h_2 &= 0 \\
e - l + h_2 &= 0.
\end{aligned} \tag{3.4}$$

Notice that in this case couplings of fermions with Φ_1 are forbidden by the $U(1)_X$ symmetry. These couplings would be allowed only if h_1 satisfies the same equations (3.4) as h_2 , implying that $h_1 = h_2$. However, since we require that $h_1 \neq h_2$, there is no value of h_1 satisfying these equations. Besides the constraints in Eqs. (3.4), anomaly freedom must also be respected. The general constraints for an anomaly free $U(1)_X$ gauge symmetry are discussed in Appendix A. It turns out that for the Type I 2HDM, the anomaly cancellation can be achieved without addition of new fermions whenever the condition $u = -2d$ is respected. To see this, we combine Equation (A.2) ($l = -3q$) with the constraints from (3.4) and write the charges of the fields as function of u and d ,

$$\begin{aligned}
q &= \frac{(u+d)}{2}, \\
l &= \frac{-3(u+d)}{2}, \\
e &= -(2u+d), \\
h_2 &= \frac{(u-d)}{2}.
\end{aligned} \tag{3.5}$$

It is then straightforward to prove that these charge assignments in Eq. (3.5) satisfy the anomaly conditions Eqs. (A.1)-(A.4). However, for the cancellation of the $[U(1)_X]^3$ term, Eq. (A.5), we find,

$$\begin{aligned}
e^3 + 3u^3 + 3d^3 - 2l^3 - 6q^3 &= [-(2u+d)]^3 + 3u^3 + 3d^3 - 2 \left[\frac{-3(u+d)}{2} \right]^3 \\
&- 6 \left[\frac{(u+d)}{2} \right]^3 \\
&= -(2u+d)^3 + 3u^3 + 3d^3 + 6(u+d)^3 \\
&= u^3 + 8d^3 + 6u^2d + 12ud^2 \\
&= (u+2d)^3.
\end{aligned} \tag{3.6}$$

This anomaly is not canceled unless $u = -2d$, i.e. if the up and down quark charges under $U(1)_X$ are proportional to their electric ones.

Here is the point at which neutrino physics can enter: if we decide to keep u and d arbitrary, the most straightforward possibility is to add right-handed neutrinos (one per generation). If their charge n is given by

$$n = -(u + 2d), \quad (3.7)$$

the $[U(1)_X]^3$ anomaly term is canceled because Eq. (A.5) becomes

$$n^3 + e^3 + 3u^3 + 3d^3 - 2l^3 - 6q^3 = -(u + 2d)^3 + (u + 2d)^3 = 0. \quad (3.8)$$

Concerning the Φ_1 charge under $U(1)_X$, we have only demanded so far that $h_1 \neq h_2$ to respect the NFC criterion, and no relation between h_1 and h_2 exist. By adding a singlet scalar to generate a Majorana mass term for the neutrinos, necessary for the implementation of the seesaw mechanism, the values of h_1 and h_2 are no longer independent, as we will see next.

3.2 Neutrino Masses

As aforementioned, in the conventional 2HDM neutrinos are massless. Similarly to the Standard Model one can simply add right-handed neutrinos and generate Dirac masses to the neutrinos. However, a compelling explanation for tiny neutrino masses arises via the seesaw mechanism [31–35]. In order to realize the type I seesaw mechanism one needs Dirac and Majorana mass terms for the neutrinos. This can be realized in our 2HDM framework by proper assignments of the quantum numbers, as we will demonstrate in what follows.

Typically, a bare mass term is introduced for the right-handed neutrinos in the realization of the seesaw mechanism without explaining its origin. Here, we explain the neutrino masses by adding a scalar singlet Φ_s , with charge h_s under $U(1)_X$. The first consequence of introducing a new singlet scalar is the extension of the scalar potential which adds to Eq. (3.1) the potential

$$V_s = m_s^2 \Phi_s^\dagger \Phi_s + \frac{\lambda_s}{2} (\Phi_s^\dagger \Phi_s)^2 + \mu_1 \Phi_1^\dagger \Phi_1 \Phi_s^\dagger \Phi_s + \mu_2 \Phi_2^\dagger \Phi_2 \Phi_s^\dagger \Phi_s + \left(\mu \Phi_1^\dagger \Phi_2 \Phi_s + h.c. \right), \quad (3.9)$$

where

$$\Phi_s = \frac{1}{\sqrt{2}} (v_s + \rho_s + i\eta_s).$$

All these terms are straightforwardly invariant under $U(1)_X$ except for the last term which requires $h_s = h_1 - h_2$. That said, the Yukawa Lagrangian involving the neutrinos reads

$$-\mathcal{L} \supset y_{ij}^D \bar{L}_{iL} \tilde{\Phi}_2 N_{jR} + Y_{ij}^M \overline{(N_{iR})^c} \Phi_s N_{Rj}, \quad (3.10)$$

Two Higgs Doublet Models free from FCNI

Fields	u_R	d_R	Q_L	L_L	e_R	N_R	Φ_2	Φ_1
Charges	u	d	$\frac{(u+d)}{2}$	$\frac{-3(u+d)}{2}$	$-(2u+d)$	$-(u+2d)$	$\frac{(u-d)}{2}$	$\frac{5u}{2} + \frac{7d}{2}$
$U(1)_A$	1	-1	0	0	-1	1	1	-1
$U(1)_B$	-1	1	0	0	1	-1	-1	1
$U(1)_C$	1/2	-1	-1/4	3/4	0	3/2	3/4	9/4
$U(1)_D$	1	0	1/2	-3/2	-2	-1	1/2	5/2
$U(1)_E$	0	1	1/2	-3/2	-1	-2	7/2	-1/2
$U(1)_F$	4/3	2/3	1	-3	-4	-8/3	1/3	17/3
$U(1)_G$	-1/3	2/3	1/6	-1/2	0	-1	-1/2	-3/2
$U(1)_{B-L}$	1/3	1/3	1/3	-1	-1	-1	0	2
$U(1)_Y$	2/3	-1/3	1/6	-1/2	-1		1/2	$\neq h_2$
$U(1)_N$	0	0	0	0	0		0	$\neq h_2$

Table 2: The first block of models are capable of explaining neutrino masses and the absence of flavor changing interactions in the 2HDM type I, whereas the second block refer to models where only the flavor problem is addressed. The first block accounts for type I 2HDM in which right-handed neutrinos are introduced without spoiling the NFC criterion ($h_1 \neq h_2$). This is possible when $u \neq -2d$ (see Eq. (3.5) and Eq. (3.14)). Conversely, the second block shows Type I 2HDM with $u = -2d$. To preserve the NFC criterion, right-handed neutrinos can not be introduced while at the same time h_1 is kept as a free parameter. The $U(1)_N$ models leads to a fermiophobic Z' setup [30]. The $U(1)_Y$ yields a "right-handed-neutrino-phobic" Z' boson. The $U(1)_{B-L}$ is the well-known model in which the accidental baryon and lepton global symmetries are gauged. The $U(1)_{C,G}$ models feature null couplings to right-handed charged leptons, whereas the $U(1)_{A,B}$ models have vanishing couplings to left-handed leptons. The $U(1)_D$ has null couplings to right-handed down-quarks. The $U(1)_{E,F}$ models induce Z' interactions to all fermions, but have rather exotic $U(1)_X$ charges.

which leads to the usual type I seesaw mechanism equation

$$(\nu N) \begin{pmatrix} 0 & m_D \\ m_D^T & M_R \end{pmatrix} \begin{pmatrix} \nu \\ N \end{pmatrix} \quad (3.11)$$

with $m_\nu = -m_D^T \frac{1}{M_R} m_D$ and $m_N = M_R$, as long as $M_R \gg m_D$, where $m_D = \frac{y^D v_2}{2\sqrt{2}}$ and $M_R = \frac{y^M v_s}{2\sqrt{2}}$. We take v_s to be at the TeV scale, and in this case $y^D \sim 10^{-4}$ and $y^M \sim 1$ lead to $m_\nu \sim 0.1$ eV in agreement with current data [36]. In this scenario right-handed neutrinos have masses at around 300 – 400 GeV, although smaller right-handed neutrino masses are also possible.

Let us now take a closer look at Eq. (3.10). Gauge invariance of the first term

requires

$$-l - h_2 + n = 0. \quad (3.12)$$

Using Eq. (3.5) and Eq. (3.7) we get

$$-l - h_2 + n = - \left[\frac{-3(u+d)}{2} \right] - \left[\frac{(u-d)}{2} \right] - (u+2d) = 0. \quad (3.13)$$

Therefore, the condition in Eq. (3.12) is automatically fulfilled. However, the Majorana mass term in Eq. (3.10) is gauge invariant if $2n + h_s = 0$, which implies from Eq. (3.7) that $h_s = 2u + 4d$. Using that $h_s = h_1 - h_2$ from the term $\mu \Phi_1^\dagger \Phi_2 \Phi_s$ in the scalar potential Eq. (3.9), we get

$$h_1 = \frac{5u}{2} + \frac{7d}{2}. \quad (3.14)$$

Now the Φ_1 charge under $U(1)_X$ is generally determined so that neutrino masses are generated. If we happened to choose $u = d = 1/3$, then $h_s = h_1 = 2$, $h_2 = 0$, and the $U(1)_X$ symmetry is identified to be $U(1)_{B-L}$ symmetry, which is spontaneously broken when Φ_s gets a vacuum expectation value. Various other choices of the charges are possible, see Table 2 for a list. From the list, the $U(1)_{B-L}$, $U(1)_N$ have been previously investigated in the literature in different contexts [37–48].

The spontaneous symmetry breaking pattern from high to low energy goes as follows: (i) the vev v_s sets the scale which the $U(1)_X$ symmetry is broken, say TeV; (ii) then v_2 breaks the $SU(2)_L \otimes U(1)_Y$ group to Quantum Electrodynamics. As for the v_1 scale, there is some freedom, but it should be either comparable to v_2 or smaller, as long as $v^2 = v_2^2 + v_1^2$, where $v = 246$ GeV, since $M_W^2 = g^2 v^2 / 4$ (see Appendix B). In the regime in which $v_s > v_2 > v_1$ one needs to tune down the g_X coupling in order to have a Z' boson that is lighter than the SM Z , which is the regime we will focus in here.

In summary, the introduction of a new gauge symmetry with the charge assignments as exhibited in Table 2 leads to a compelling solution to the flavor problem in the Type I 2HDM, while successfully generating fermion masses. In particular, neutrino masses are explained via the seesaw mechanism. A similar reasoning, respecting the NFC criterion ($h_1 \neq h_2$), can be applied to other types of 2HDM preventing them of FCNI. Nevertheless, the addition of extra chiral fermions is required to preserve them free of anomalies. Therefore, we focus in this paper on 2HDM of Type I, see Table 2.

Now that we have reviewed the theoretical motivations for introducing an Abelian symmetry to the framework of the 2HDM we discuss in model detail the spectrum of the gauge bosons and neutral currents.

3.3 Physical Gauge Bosons and Neutral Currents

We emphasize that we are including all renormalizable terms allowed guided by gauge invariance. Therefore, kinetic mixing between the two Abelian groups is present. To understand the impact of kinetic mixing in the determination of the physical gauge boson we should start off writing down the kinetic terms of the gauge bosons. Note that throughout, the kinetic mixing parameter should fulfill $\epsilon \ll 1$ to be consistent with precision electroweak constraints. That said, the most general gauge Lagrangian associated to these groups is [49–51]:

$$\mathcal{L}_{\text{gauge}} = -\frac{1}{4}\hat{B}_{\mu\nu}\hat{B}^{\mu\nu} + \frac{\epsilon}{2\cos\theta_W}\hat{X}_{\mu\nu}\hat{B}^{\mu\nu} - \frac{1}{4}\hat{X}_{\mu\nu}\hat{X}^{\mu\nu}, \quad (3.15)$$

with the following covariant derivative

$$D_\mu = \partial_\mu + igT^a W_\mu^a + ig'\frac{Q_Y}{2}\hat{B}_\mu + ig_X\frac{Q_X}{2}\hat{X}_\mu. \quad (3.16)$$

Here T^a , W_μ^a and g are the generators, gauge bosons and gauge coupling constant of $SU(2)_L$ respectively; \hat{X}_μ and \hat{B}_μ the $U(1)_X$ and $U(1)_Y$ gauge bosons, g_X (Q_X) is the $U(1)_X$ coupling constant (charge) and g' (Q_Y) is $U(1)_Y$ coupling constant (charge). The hats means that they are non-physical, i.e. yet to be diagonalized, fields. As usual $\hat{B}_{\mu\nu} = \partial_\mu\hat{B}_\nu - \partial_\nu\hat{B}_\mu$ and $\hat{X}_{\mu\nu} = \partial_\mu\hat{X}_\nu - \partial_\nu\hat{X}_\mu$.

One first performs a so-called $GL(2, \mathbb{R})$ rotation in order to make the kinetic terms canonical,

$$\begin{pmatrix} X_\mu \\ B_\mu \end{pmatrix} = \begin{pmatrix} \sqrt{1 - (\epsilon/\cos\theta_W)^2} & 0 \\ -\epsilon/\cos\theta_W & 1 \end{pmatrix} \begin{pmatrix} \hat{X}_\mu \\ \hat{B}_\mu \end{pmatrix}. \quad (3.17)$$

Therefore $\hat{B}_\mu = \eta_X X_\mu + B_\mu$, and $\hat{X}_\mu = X_\mu$, where

$$\eta_X = \frac{\epsilon/\cos\theta_W}{\sqrt{1 - (\epsilon/\cos\theta_W)^2}} \simeq \epsilon/\cos\theta_W, \quad (3.18)$$

since we are taking $\epsilon/\cos\theta_W \ll 1$ throughout. Thus, the covariant derivative now reads,

$$D_\mu = \partial_\mu + igT^a W_\mu^a + ig'\frac{Q_Y}{2}B_\mu + \frac{i}{2}\left(g_X Q_X + g'\frac{\epsilon}{\cos\theta_W}Q_Y\right)X_\mu. \quad (3.19)$$

which is from where we derive the gauge boson masses.

The general formalism of diagonalizing the neutral gauge boson mass matrix is delegated to Appendix B. The gauge boson mixing is parametrized in terms of ϵ_Z and ϵ , coming from the contributions of the second Higgs doublet and the kinetic mixing between the $U(1)$ groups respectively (see below and (B.32)). In the regime

in which the new vector boson is much lighter than the SM Z boson, we get two mass eigenstates; one identified as the SM Z boson, labeled Z^0 with, $m_{Z^0}^2 = \frac{g^2 v^2}{4 \cos^2 \theta_W}$ and the Z' boson with,

$$m_{Z'}^2 = \frac{v_s^2}{4} g_X^2 q_X^2 + \frac{g_X^2 v^2 \cos^2 \beta \sin^2 \beta}{4} (Q_{X1} - Q_{X2})^2, \quad (3.20)$$

where q_X , Q_{X1} , Q_{X2} are the charges under $U(1)_X$ of the singlet scalar, Higgs doublets Φ_1 and Φ_2 respectively, $\tan \beta = v_2/v_1$, $v = \sqrt{v_1^2 + v_2^2} = 246$ GeV, v_s sets the $U(1)_X$ scale of spontaneous symmetry breaking, and g_X is the coupling constant of the $U(1)_X$ symmetry.

It will be useful to write the Z' mass in a compact form as (see Appendix C) by defining $\tan \beta_d = \frac{v_s}{v_1}$ as follows,

$$m_{Z'} = \frac{g_X v \cos^2 \beta}{\delta}, \quad (3.21)$$

where

$$\delta = \frac{2 \cos \beta \cos \beta_d}{\sqrt{q_X^2 + \cos^2 \beta_d (\sin^2 \beta (Q_{X1} - Q_{X2})^2 - q_X^2)}}. \quad (3.22)$$

The mixing angle for the diagonalization of the gauge bosons, ξ , in this general setup can be parametrized as follows (see (B.29)),

$$\xi \equiv \epsilon_Z + \epsilon \tan \theta_W, \quad (3.23)$$

where,

$$\epsilon_Z \equiv \frac{g_X}{g_Z} (Q_{X1} \cos^2 \beta + Q_{X2} \sin^2 \beta). \quad (3.24)$$

For instance, in the $B - L$ model one has,

$$\epsilon_Z = 2 \frac{g_X}{g} \cos^2 \beta, \quad (3.25)$$

and with the use of Eq. (3.21) we get,

$$\delta = \frac{m_Z}{m_{Z'}} \epsilon_z, \quad (3.26)$$

which agrees with [41], validating our findings.

Having obtained the physical fields we can rewrite the neutral current Lagrangian (see Appendices B and D):

$$\begin{aligned} \mathcal{L}_{\text{NC}} = & -e J_{\text{em}}^\mu A_\mu - \frac{g}{2 \cos \theta_W} J_{\text{NC}}^\mu Z_\mu - \left(\epsilon e J_{\text{em}}^\mu + \epsilon_Z \frac{g}{2 \cos \theta_W} J_{\text{NC}}^\mu \right) Z'_\mu \\ & + \frac{1}{4} g_X \sin \xi \left[(Q_{Xf}^R + Q_{Xf}^L) \bar{\psi}_f \gamma^\mu \psi_f + (Q_{Xf}^R - Q_{Xf}^L) \bar{\psi}_f \gamma^\mu \gamma_5 \psi_f \right] Z_\mu \\ & - \frac{1}{4} g_X \cos \xi \left[(Q_{Xf}^R + Q_{Xf}^L) \bar{\psi}_f \gamma^\mu \psi_f - (Q_{Xf}^L - Q_{Xf}^R) \bar{\psi}_f \gamma^\mu \gamma_5 \psi_f \right] Z'_\mu, \end{aligned} \quad (3.27)$$

where Q_X^R (Q_X^L) are the left-handed (right-handed) fermion charges under $U(1)_X$. We emphasize that Eq. (3.27) is the general neutral current for 2HDM augmented by a $U(1)_X$ gauge symmetry.

Again, it is important to validate our results with the existing literature. For instance, in the $U(1)_{B-L}$ model we get

$$\begin{aligned} \mathcal{L}_{\text{NC}} = & -eJ_{\text{em}}^\mu A_\mu - \frac{g}{2\cos\theta_W} J_{\text{NC}}^\mu Z_\mu - \left(\epsilon e J_{\text{em}}^\mu + \epsilon_Z \frac{g}{2\cos\theta_W} J_{\text{NC}}^\mu \right) Z'_\mu \\ & - \frac{g_X}{2} Q_{Xf} [\bar{\psi}_f \gamma^\mu \psi_f] Z'_\mu, \end{aligned} \quad (3.28)$$

where $Q_{Xf} = -1$ for charged leptons and $Q_{Xf} = 1/3$ for quarks, with g_X and ϵ_Z related by Eq. (3.25), in agreement with [52].

Now that we have obtained the neutral current for a generic $U(1)_X$ model in the context of the 2HDM we will address the relevant constraints these $U(1)_X$ models are subject to.

3.4 Z' Decays

We have introduced a multitude of Abelian gauge groups in the context of the 2HDM that address two major issues in the original 2HDM framework, namely the absence of neutrino masses and the presence of flavor changing interactions. Abelian groups generally give rise to neutral gauge bosons which are subject to a rich phenomenology that we plan to explore in what follows. Before doing so, some general remarks are in order:

- (i) The kinetic mixing (ϵ) as well as the mass mixing (ϵ_Z) parameters are required to be smaller than 10^{-3} to be consistent with a variety of constraints that we will discuss.
- (ii) We will focus on the regime $m_{Z'} \ll m_Z$, say $m_{Z'} = 1 \text{ MeV} - 10 \text{ GeV}$. Some comments on different regimes will nevertheless be made whenever relevant.
- (iii) A light Z' can be achieved at the expense of tuning the gauge coupling g_X .
- (iv) The phenomenology of our models will be dictated by either the kinetic mixing or the mass-mixing terms.

That said, some of the constraints we will investigate are based on dark photon searches. Notice that our models are a bit different than the dark photon model that has only the kinetic mixing term, due to the presence of mass-mixing and the non-vanishing $U(1)_X$ charges of the SM fermions. We remind the reader that only the models that simultaneously explain neutrino masses and free the 2HDM from

flavor changing interactions are of interest throughout this work, as displayed in the first block of Table 2. With this in mind we discuss the Z' decays in each one of the models.

- It is important to first mention the dark photon model. In such models the coupling of the dark photon A' with SM fermions f goes as $\bar{f}\gamma^\mu f A'_\mu$. The corresponding branching ratios are shown in Fig. 1. It is important to have a clear picture of the dark photon model because some of the bounds discussed in this work have the dark photon model as benchmark as we shall see when we address neutrino-electron scattering and low energy accelerator constraints.
- In the $U(1)_A$ model, the charged leptons and light quarks charges under $U(1)_A$ are the same but due to color multiplicity the Z' decays mostly into light quarks as shown in Fig. 1. As for the $U(1)_B$ model, the results are same. Notice that the label B has nothing to do with baryon number. No decays into active neutrinos exist since the lepton doublet is uncharged under the new gauge group.
- In the $U(1)_C$ model, the branching ratio into neutrinos is more relevant in comparison with previous models since now the lepton doublet has charge 3/4 under the new gauge group. However, decays into light quarks are still the most relevant. The $U(1)_G$ model has a similar behavior.
- In the $U(1)_D$ model, the branching ratio into leptons prevails. A similar feature happens in the $U(1)_{B-L}$ model, where B and L account for the baryon and lepton numbers. In the former, the branching ratios into charged fermions and neutrinos are very similar, but as soon the decay into muons becomes kinematically accessible the branching ratio into charged leptons increases. In the latter, decays into neutrinos are always dominant in the mass region of interest, as a straightforward consequence of the baryon and lepton quantum numbers of the fermions.
- In the $U(1)_E$ model, decays into neutrinos are dominant until the Z' mass approximates the strange quark and muon kinematic thresholds.

Now that we have highlighted the properties of the Z' gauge boson for each $U(1)_X$ model we will discuss a variety of constraints going from mesons decays to low energy accelerators.

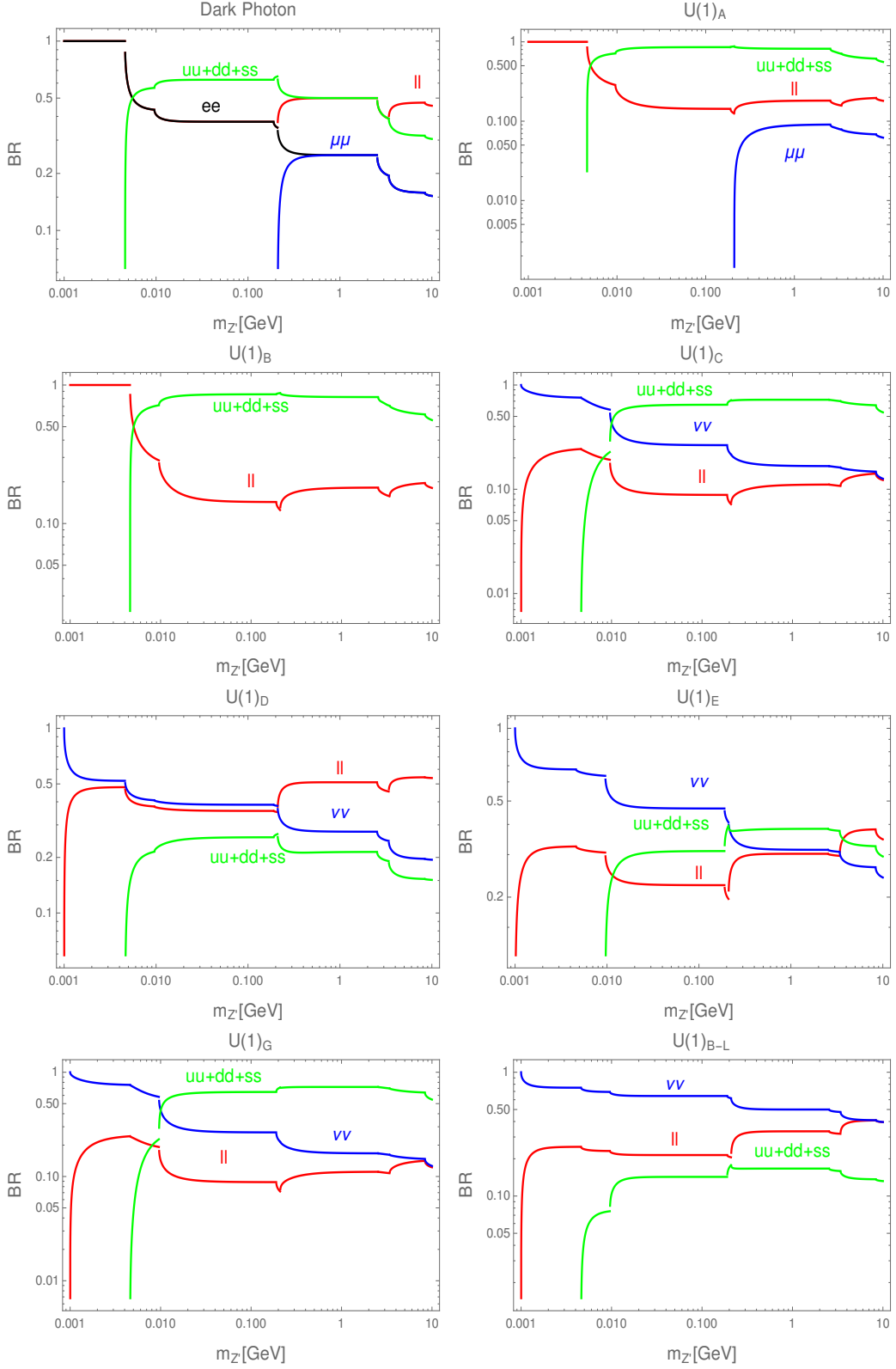


Figure 1: Branching ratios as a function of the Z' mass for several $U(1)_X$ models under study.

4 Phenomenological Constraints

In this section we will span over the existing limits on the $U(1)_X$ models proposed previously. Our main goal is to estimate limits on the parameter space of these models and assess how relevant they are. A more dedicated study will be conducted elsewhere. We start with meson decays.

4.1 Meson Decays

4.1.1 Rare K Decays

The main decays modes of the charged Kaon are $\mu\nu_\mu$, $\pi^+\pi^0$ and $\pi^+\pi^+\pi^0$ with branching ratios of 64%, 21% and 6% respectively. Searches for rare meson decays such as $K^+ \rightarrow \pi^+l^+l^-$ have also been performed [53, 54], which led to the experimental constraints [24],

$$\text{BR}(K^+ \rightarrow \pi^+e^+e^-)_{\text{exp}} = (3.00 \pm 0.09) \times 10^{-7}, \quad (4.1)$$

$$\text{BR}(K^+ \rightarrow \pi^+\mu^+\mu^-)_{\text{exp}} = (9.4 \pm 0.6) \times 10^{-8}, \quad (4.2)$$

$$\text{BR}(K^+ \rightarrow \pi^+\nu\bar{\nu})_{\text{exp}} = (1.7 \pm 1.1) \times 10^{-10}. \quad (4.3)$$

In a Two Higgs Doublet Model with $Z - Z'$ mass mixing the branching ratio of $K^+ \rightarrow \pi^+Z'$ is estimated to be [55],

$$\text{BR}(K^+ \rightarrow \pi^+Z') \simeq 4 \times 10^{-4} \delta^2, \quad (4.4)$$

where $\delta = \epsilon_Z m_Z / m_{Z'}$ (see Appendix C). Comparing Eq. (4.4) with Eqs. (4.1)-(4.3) we conservatively find that,

$$\delta \lesssim \frac{2 \times 10^{-2}}{\sqrt{\text{BR}(Z' \rightarrow l^+l^-)}}, \quad (4.5)$$

$$\delta \lesssim \frac{7 \times 10^{-4}}{\sqrt{\text{BR}(Z' \rightarrow \text{missing energy})}}. \quad (4.6)$$

These bounds should be used with care since they are not applicable to any Z' mass. For instance, the bound obtained in Eq. (4.1) was obtained with a hard cut in the dilepton invariant mass, namely $m_{ee} > 140$ MeV [54]. Thus this limit is valid for $m_{Z'} > 140$ MeV.

In the $U(1)_{B-L}$ model, for instance, for $m'_Z < 2m_\mu$, the Z' decays with $\sim 75\%$ branching ratio into neutrinos and therefore Eq. (4.6) should be used, giving stronger constraints. In the $U(1)_N$ model, on other hand, the situation strongly depends on the ratio ϵ/ϵ_Z . In particular, for $\epsilon/\epsilon_Z \gg 1$, the Z' decays mostly into charged leptons with Eq. (4.5) yielding stronger limits, conversely for $\epsilon/\epsilon_Z < 1$, Eq. (4.6) is more restrictive in agreement with [38]. Either way it is clear that rare kaon decays introduce an interesting pathway to probe new physics, specially low mass Z' gauge bosons [56–60].

<i>K</i> Decays	
$\delta \lesssim 2 \times 10^{-2} / \sqrt{BR(Z' \rightarrow l^+l^-)}$	
$\delta \lesssim 7 \times 10^{-4} / \sqrt{BR(Z' \rightarrow \text{missing energy})}$	
<i>B</i> Decays	
$\delta \lesssim 2 \times 10^{-3} / \sqrt{BR(Z' \rightarrow l^+l^-)}$	
$\delta \lesssim 1.2 \times 10^{-2} / \sqrt{BR(Z' \rightarrow \text{missing energy})}$	

Table 3: Summary of constraints on the model from meson decays.

4.1.2 Rare *B* Decays

Similar to the *K* mesons discussed previously rare *B* decays offer a promising environment to probe new physics. In particular, the charged *B* meson with mass of 5.3 GeV, comprised of $u\bar{b}$, may possibly decay into $K^+l^+l^-$ [61–63] or $K^+\nu\bar{\nu}$ [64, 65]. Such decays have been measured to be [24],

$$BR(B^+ \rightarrow K^+\bar{l}^+l^-)_{\text{exp}} < 4.5 \times 10^{-7}, \quad (4.7)$$

$$BR(B^+ \rightarrow K^+\nu\bar{\nu})_{\text{exp}} < 1.6 \times 10^{-5}. \quad (4.8)$$

Having in mind that the mass mixing in the 2HDM induces [38, 55, 62],

$$BR(B \rightarrow KZ_d) \simeq 0.1\delta^2, \quad (4.9)$$

implying that,

$$\delta \lesssim \frac{2 \times 10^{-3}}{\sqrt{BR(Z' \rightarrow l^+l^-)}}, \quad (4.10)$$

$$\delta \lesssim \frac{1.2 \times 10^{-2}}{\sqrt{BR(Z' \rightarrow \text{missing energy})}}. \quad (4.11)$$

Comparing Eqs. (4.10)–(4.11) with Eqs. (4.5)–(4.6) we can see the rare *B* decays give rise to more stringent limits on the parameter δ when the Z' decays mostly into charged leptons. We highlight that the large factor in Eq. (4.9) is result of the presence of the top quark in the Feynman diagram responsible for the $b \rightarrow s$ conversion, and consequently the $B \rightarrow KZ'$ decay.

As for Z' decays into neutrino pairs, then precise measurements on Kaon decays offer the leading constraints. The constraints from meson decays are summarized in Table 3. We will now move to Higgs physics.

4.2 Higgs Physics

4.2.1 Higgs Properties

Our models are comprised of two Higgs doublets and a singlet scalar. In the limit in which the scalar doublets do not mix with the singlet, i.e. the regime in which the

vertex	coupling constant
$H t\bar{t}, H b\bar{b}, H \tau\bar{\tau}$	$\frac{\sin \alpha}{\sin \beta}$
$H WW, H ZZ$	$\cos(\beta - \alpha)$
$h t\bar{t}, h b\bar{b}, h \tau\bar{\tau}$	$\frac{\cos \alpha}{\sin \beta}$
$h WW, h ZZ$	$\sin(\beta - \alpha)$

Table 4: Higgs and light scalar interactions in the 2HDM type I. The coupling constants in the second column are the overall multiplicative factor in front of the SM couplings. In other words, when $\alpha = \beta$ the Higgs in the 2HDM type I interacts with fermions and gauge bosons identically to the SM Higgs.

parameters μ_1, μ_2, μ in the potential (3.9) are suppressed, one finds [41]

$$\begin{aligned}
m_s^2 &= \lambda_s v_s^2, \\
m_h^2 &= \frac{1}{2} \left(\lambda_1 v_1^2 + \lambda_2 v_2^2 - \sqrt{(\lambda_1 v_1^2 - \lambda_2 v_2^2)^2 + 4(\lambda_3 + \lambda_4)^2 v_1^2 v_2^2} \right), \\
m_H^2 &= \frac{1}{2} \left(\lambda_1 v_1^2 + \lambda_2 v_2^2 + \sqrt{(\lambda_1 v_1^2 - \lambda_2 v_2^2)^2 + 4(\lambda_3 + \lambda_4)^2 v_1^2 v_2^2} \right),
\end{aligned} \tag{4.12}$$

where the H - h mixing is given by

$$\begin{pmatrix} H \\ h \end{pmatrix} = \begin{pmatrix} \cos \alpha & \sin \alpha \\ -\sin \alpha & \cos \alpha \end{pmatrix} \begin{pmatrix} \phi_1 \\ \phi_2 \end{pmatrix} \tag{4.13}$$

with

$$\tan 2\alpha = \frac{2(\lambda_3 + \lambda_4)v_1 v_2}{\lambda_1 v_1^2 - \lambda_2 v_2^2}. \tag{4.14}$$

Notice that in the limit $\sin \alpha \sim 1$, $H \sim \phi_2$, i.e. the SM Higgs, and $h \sim \phi_1$. Moreover, it is clear from Eq. (4.12) that in the 2HDM we are considering the SM-like Higgs is heavier than the light scalar h . Their interactions strength with SM particles is summarized in Table 4. The couplings constants in the second column of the table are multiplicative factors appearing in front of the SM couplings. In other words, when $\alpha = \beta$ the Higgs in the 2HDM type I interacts with fermions and gauge bosons identically to the SM Higgs. Furthermore, the regime $\beta \sim \alpha$ renders the $h t\bar{t}$, $h b\bar{b}$ and $h \tau\bar{\tau}$ couplings governed by $\cot \beta$, whereas the $h WW$, $h ZZ$ interactions are dwindled.

4.2.2 Higgs Associated Production

Several experiments have searched for scalars with similar properties to the SM Higgs at LEP. They were particularly focused on the associated production with the Z boson, with the scalar decaying either into fermions or invisibly as displayed in Fig. 2. The light Higgs in the models under study, h , decays at tree-level into $Z'Z'$. Since the

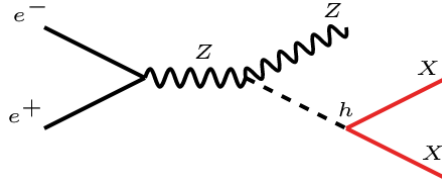


Figure 2: Higgs associated production at LEP followed by its invisible decay, illustrated by $h \rightarrow XX$.

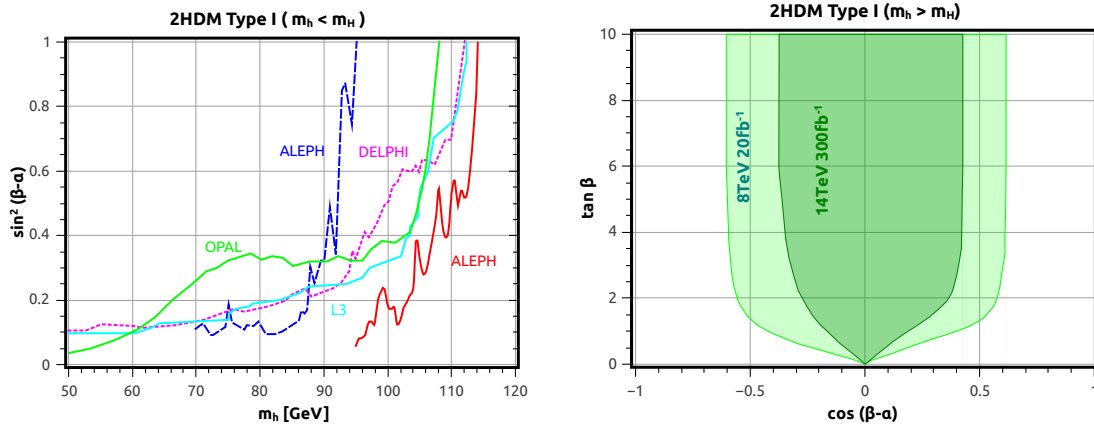


Figure 3: Left-panel: Upper limits from invisible Higgs decay searches translated to the light Higgs mass m_h . Right-panel: Constraints from the LHC on the Higgs properties in the context of 2HDM type I with $m_h > m_H$, where H is the SM Higgs, a scenario which is opposite to what it is being considered here.

LEP searches did not cover fermions with very small invariant mass, i.e. stemming from a light Z' , one should use the results from the invisible decay search. That said, the Zh associated production search resulted into limits on the product of the production cross section strength and branching ratio, i.e. $\sigma(Zh)/\sigma(ZH_{SM})BR(h \rightarrow \text{inv})$.

Assuming $BR(h \rightarrow \text{inv}) \simeq 1$ throughout, one can reinterpret the results from [66–68] for the light Higgs h , having in mind that the hZZ coupling goes with $\sin(\beta - \alpha)$, to place a bound on $\sin^2(\beta - \alpha)$ as a function of the scalar mass as shown in the left panel of Fig. 3 [41]. From Fig. 3, one can conservatively conclude that $\sin^2(\beta - \alpha) \lesssim 0.1$, $\cos^2(\beta - \alpha) > 0.9$, independent of $\tan \beta$. Weaker limits are applicable depending on the light Higgs mass.

However, the limit presented in Fig. 3 may be not robust because it relies on the assumption that $BR(h \rightarrow \text{inv}) \simeq 1$. A simple check can be done by comparing the decay into $Z'Z'$ with the usually dominant $b\bar{b}$ mode that lead to the following decay

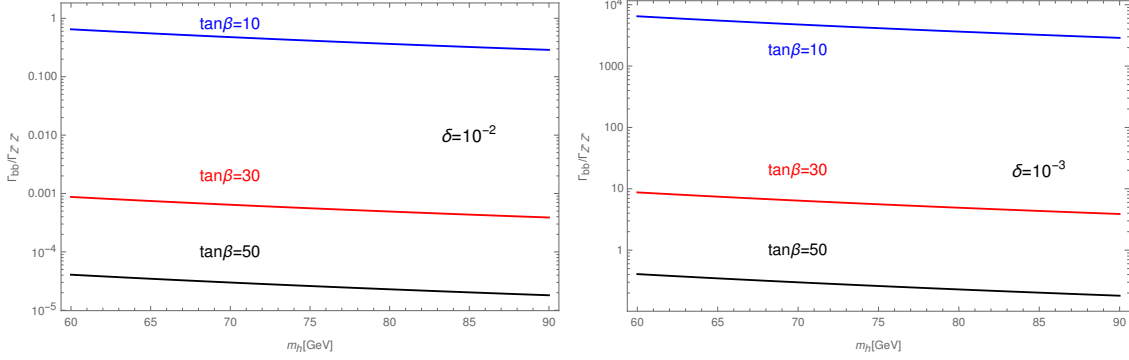


Figure 4: Ratio of the light Higgs decay width for different values of $\tan \beta$. In the left panel we set $\delta = 10^{-2}$, while in the right one $\delta = 10^{-3}$. One can see that if the product $\delta \tan \beta$ is sufficiently small, the light Higgs decays dominantly into $Z'Z'$. In this regime, the limits presented in the left panel of Fig. 3 can be directly applied.

rates,

$$\Gamma_{h \rightarrow Z'Z'} = \frac{g_Z^2}{128\pi} \frac{m_h^3}{m_Z^2} (\delta \tan \beta)^4 \left(\frac{\cos^3 \beta \cos \alpha - \sin^3 \beta \sin \alpha}{\cos \beta \sin \beta} \right)^2, \quad (4.15)$$

$$\Gamma_{h \rightarrow b\bar{b}} = \frac{3m_b^2 m_h}{8\pi v^2} \left(\frac{\cos \alpha}{\sin \beta} \right)^2. \quad (4.16)$$

We thus conclude that the ratio reads

$$\frac{\Gamma_{h \rightarrow b\bar{b}}}{\Gamma_{h \rightarrow Z'Z'}} = \frac{12m_b^2}{m_h^2} \frac{1}{(\delta \tan \beta)^4} \left(\frac{\cos \beta \sin \beta}{\cos^3 \beta \cos \alpha - \sin^3 \beta \sin \alpha} \right)^2 \left(\frac{\cos \alpha}{\sin \beta} \right)^2, \quad (4.17)$$

which is displayed in Fig. 4, where we plot this ratio for different values of $\tan \beta$ as a function of the light Higgs mass. In the left panel we fix $\delta = 10^{-2}$, whereas in the right one $\delta = 10^{-3}$. One can see that if the product $\delta \tan \beta$ is sufficiently small, the light Higgs decays dominantly into $Z'Z'$, as predicted by Eq. (4.16), justifying our procedure in the derivation of Fig. 3. A more detailed study regarding the light Higgs properties has been conducted elsewhere [41]. In this work, we are limited to discuss all relevant limits to the $U(1)_X$ models introduced above.

For completeness, in the right panel of Fig. 3, we exhibit the limits from LHC data for the 2HDM type I, assuming that the light Higgs is instead the SM Higgs, i.e. $m_h > m_H$, whose interactions strength with gauge bosons is proportional $\cos(\beta - \alpha)$. The SM limit in this case is found when $\beta \sim \alpha + \pi/2$, where $H \sim \phi_1$ and $h \sim \phi_2$. Fig. 3 is still useful to us though, because it shows that for $\tan \beta > 1$ larger deviations from the SM Higgs are allowed. Moreover, we indeed assume $v_2 > v_1$, thus $\tan \beta > 1$, throughout.

Higgs decay channel	branching ratio	error
$b\bar{b}$	5.84×10^{-1}	1.5%
$c\bar{c}$	2.89×10^{-2}	6.5%
$g g$	8.18×10^{-2}	4.5%
ZZ^*	2.62×10^{-1}	2%
WW^*	2.14×10^{-1}	2%
$\tau^+\tau^-$	6.27×10^{-2}	2%
$\mu^+\mu^-$	2.18×10^{-4}	2%
$\gamma\gamma$	2.27×10^{-3}	2.6%
$Z\gamma$	1.5×10^{-3}	6.7%
$ZZ^* \rightarrow 4\ell$	2.745×10^{-4}	2%
$ZZ^* \rightarrow 2\ell 2\nu$	1.05×10^{-4}	2%

Table 5: List of experimental limits on the branching ratio of the SM Higgs. The channel $ZZ^* \rightarrow 2\ell 2\nu$ was obtained using the relation $BR(H \rightarrow ZZ^* \rightarrow 2\ell 2\nu) = BR(H \rightarrow ZZ^*)BR(Z \rightarrow 2\ell)BR(Z \rightarrow 2\nu)^2$.

4.2.3 Higgs Decays

After the Higgs discovery the LHC has turned into a Higgs factory and today we have at our disposal much better measurements of the Higgs branching ratio (see Table 5). Since we are mostly interested in the regime in which the Z' is light enough for the Higgs to decay into, some channels are of great interest for our purposes, namely $H \rightarrow ZZ^* \rightarrow 4\ell$ and $H \rightarrow ZZ^* \rightarrow 2\ell 2\nu$. In the context of 2HDM it has been shown that in the limit in which the Z' gauge boson is much lighter than the Z boson we get [41],

$$\Gamma(H \rightarrow ZZ') = \frac{g_Z^2}{64\pi} \frac{(M_H^2 - M_Z^2)^3}{M_H^3 M_Z^2} \delta^2 \tan \beta^2 \sin^2(\beta - \alpha), \quad (4.18)$$

and

$$\Gamma(H \rightarrow Z'Z') = \frac{g_Z^2}{128\pi} \frac{M_H^3}{M_Z^2} \delta^4 \tan \beta^4 \left(\frac{\cos^3 \beta \sin \alpha + \sin^3 \beta \cos \alpha}{\cos \beta \sin \beta} \right)^2. \quad (4.19)$$

One can now use precision measurements on Higgs properties summarized in Table 5 to constrain the model. We will focus on the decay into ZZ' since δ is supposed to be small to obey meson decay constraints¹. Enforcing the branching ratio $\Gamma(H \rightarrow ZZ' \rightarrow 4\ell)/\Gamma_{\text{total}}$ with $\Gamma_{\text{total}} = 4.1 \text{ MeV}$, to match the measured value within the error bars as indicated in the Table 5 we obtain,

$$\delta^2 \leq \frac{4.6 \times 10^{-6}}{BR(Z' \rightarrow l^+l^-) \sin^2(\beta - \alpha) \tan \beta^2}. \quad (4.20)$$

¹In some regions of the parameter space with sufficiently large $\tan \beta$ the decay $Z'Z'$ might become relevant as discussed in [41].

To have an idea on how competitive this constraint is compared to previous discussions we shall plug in some numbers. Taking $\sin^2(\beta - \alpha) = 0.01$ and $\tan \beta = 10$, we get

$$\delta \leq \frac{0.002}{\sqrt{BR(Z' \rightarrow l^+l^-)}}, \quad (4.21)$$

which is comparable to the bound stemming from Kaon decays. We emphasize that this bound is applicable to all $U(1)_X$ models under study here. One need now to simply choose a model and substitute the respective branching ratio into charged leptons as provided by Fig. 1.

4.3 Z Decays

In the models we are investigating both the light Higgs h and the Z' can be much lighter than the Z , kinematically allowing the decay $Z \rightarrow hZ'$. In the limit that the Z' mass is very small compared to the Z mass we find,

$$\Gamma(Z \rightarrow hZ') = (\mathcal{C}_{h-Z-Z'})^2 \frac{m_Z}{64\pi m_{Z'}^2} \left(1 - \frac{m_h^2}{m_Z^2}\right)^3. \quad (4.22)$$

where (see Appendix F)

$$\mathcal{C}_{h-Z-Z'} = g_Z g_X v \cos \beta \sin \beta \cos(\beta - \alpha). \quad (4.23)$$

Knowing that we can write down the Z' mass as a function of δ , as derived in Appendix C, we get

$$\Gamma(Z \rightarrow hZ') = \frac{g_Z^2 m_Z}{64\pi} (\delta \tan \beta)^2 \cos^2(\beta - \alpha) \left(1 - \frac{m_h^2}{m_Z^2}\right)^3. \quad (4.24)$$

We highlight that the exact expression for this decay depends on the Φ_1 charge under $U(1)_X$. Eq. (4.24) is valid for the $B - L$ model for instance, and it agrees with [41]. Anyways, knowing that the total decay width of the Z is $\Gamma_Z = 2.4952 \pm 0.0023$ GeV [69], one can conservatively enforce the new physics decay to be within the error bars of the measured value. One can use this to place a lower mass limit on m_h as a function of $\delta \tan \beta$ taking $\cos^2(\beta - \alpha) \sim 0.9 - 1$ as shown in Fig. 5.

One can conclude that for sufficiently small $\delta \tan \beta$ the bounds from LEP substantially weaken. We have seen in the previous sections that $\delta < 10^{-2} - 10^{-3}$, and since we are interested in the limit of large $\tan \beta$, say $\tan \beta \sim 10$, then the light Higgs in the $U(1)_X$ models under study can be arbitrarily light as long as a fine-tuning in Eq. (4.12) is invoked. It has been noted that if $\sin \alpha$ is different from unity, m_h cannot be lighter than $m_H/2$, otherwise the heavy Higgs, i.e. the SM Higgs, would decay dominantly into hh in strong disagreement with data [70]. Thus this very light Higgs scenario is only possible in the limit $\sin \alpha = 1$.

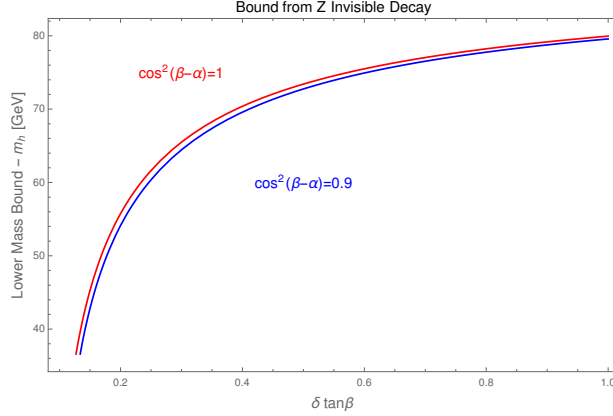


Figure 5: Lower mass bound on the light Higgs stemming from the LEP precision measurement on the Z width.

4.4 Charged Higgs Searches

A pleasant feature of our framework is that in contrast to canonical 2HDM there is no pseudoscalar Higgs particle², as this degree of freedom becomes the longitudinal polarization of the Z' . However, it certainly does have a charged scalar, H^\pm , which is orthogonal to the longitudinal component of the W^\pm . The phenomenology of the charged Higgs in the ordinary Type I model was recently discussed in Ref. [4].

In 2HDM type I, the coupling of the charged Higgs to fermions is suppressed by a factor of $\tan\beta$. In the models under study, the charged Higgs mass is found to be $m_{H^\pm}^2 = \frac{\lambda_4}{2}v^2$. This mass determines which final state is dominant in its decays [4, 71–74]. In this work we will adopt $\lambda_4 \sim 1$, and in this case the hW , HW and $t\bar{b}$ decays are the dominant ones and are found to be described by [75, 76]

$$\Gamma(H^\pm \rightarrow hW^\pm) = \frac{\cos^2(\beta - \alpha)}{16\pi v^2} \frac{1}{m_{H^\pm}^3} \lambda^{3/2}(m_{H^\pm}^2, m_h^2, m_W^2) \quad (4.25)$$

with $\lambda(x, y, z) \equiv x^2 + y^2 + z^2 - 2xy - 2yz - 2zx$,

$$\Gamma(H^\pm \rightarrow HW^\pm) = \frac{\sin^2(\beta - \alpha)}{16\pi v^2} \frac{1}{m_{H^\pm}^3} \lambda^{3/2}(m_{H^\pm}^2, m_H^2, m_W^2), \quad (4.26)$$

and the decay width into $t\bar{b}$ is given by

$$\Gamma(H^\pm \rightarrow t\bar{b}) \simeq \frac{3m_{H^\pm}}{8\pi v^2} \frac{m_t^2}{\tan^2\beta} \left(1 - \frac{m_t^2}{m_{H^\pm}^2}\right)^2 \quad (4.27)$$

²There is a pseudoscalar associated with a Higgs singlet, which remains decoupled as we assume no mixing between the doublets and singlet. When sizable mixing is introduced, the remaining pseudoscalar would have small couplings to the SM particles and it could be in principle detectable.

Experiment	$\langle Q \rangle$	$\sin^2 \theta_W(m_Z)$	Bound on dark Z (90% CL)
Cesium APV	2.4 MeV	0.2313(16)	$\varepsilon^2 < \frac{39 \times 10^{-6}}{\delta^2} \left(\frac{m_{Z_d}}{m_Z} \right)^2 \frac{1}{K(m_{Z_d})^2}$
E158 (SLAC)	160 MeV	0.2329(13)	$\varepsilon^2 < \frac{62 \times 10^{-6}}{\delta^2} \left(\frac{(160 \text{ MeV})^2 + m_{Z_d}^2}{m_Z m_{Z_d}} \right)^2$
Qweak (JLAB)	170 MeV	± 0.0007	$\varepsilon^2 < \frac{7.4 \times 10^{-6}}{\delta^2} \left(\frac{(170 \text{ MeV})^2 + m_{Z_d}^2}{m_Z m_{Z_d}} \right)^2$
Moller (JLAB)	75 MeV	± 0.00029	$\varepsilon^2 < \frac{1.3 \times 10^{-6}}{\delta^2} \left(\frac{(75 \text{ MeV})^2 + m_{Z_d}^2}{m_Z m_{Z_d}} \right)^2$
MESA (Mainz)	50 MeV	± 0.00037	$\varepsilon^2 < \frac{2.1 \times 10^{-6}}{\delta^2} \left(\frac{(50 \text{ MeV})^2 + m_{Z_d}^2}{m_Z m_{Z_d}} \right)^2$

Table 6: Existing (Cesium, E158) and projected constraints on the kinetic mixing parameter as a function of the mass mixing parameter δ and the Z' mass. All masses are in MeV, hence $m_Z = 91000$ MeV.

where we have taken $V_{tb} = 1$.

The constraints coming from charged Higgs bosons searches are not very restrictive and in the limit of large $\tan \beta$ as assumed in this work, charged Higgs searches do not yield competitive limits and thus ignored henceforth. For a detailed discussion see [77].

4.5 Atomic Parity Violation

The search for Atomic Parity Violation (APV) provides a promising pathway to probe new physics, especially the existence of neutral light bosons. It is known that for $m_{Z'} \sim 0.1 - 1$ GeV, existing limits exclude $\varepsilon^2 > 10^{-6}$ [44]. As we shall see in what follows, APV offers an orthogonal and complementary probe for new physics depending on the parameter δ .

Anyways, this parity violation is two fold: (i) it can be induced via the non-zero SM fermion charges under the $U(1)_X$ symmetry; (ii) it can arise via the $Z' - Z$ mass mixing. That said, let us first review how one can constrain $U(1)_X$ models via atomic parity violation. Using effective field theory APV is parametrized as [78]

$$\begin{aligned}
- \mathcal{L}_{\text{eff}} = & \frac{g^2 + g'^2}{m_Z^2} \frac{1}{4} \bar{e} \gamma_\mu \gamma_5 e \left[\left(\frac{1}{4} - \frac{2}{3} s_W^2 \right) \bar{u} \gamma^\mu u + \left(-\frac{1}{4} + \frac{1}{3} s^2 \right) \bar{d} \gamma^\mu d \right] \\
& - \frac{f_{Ae}}{m_{Z'}^2} \bar{e} \gamma_\mu \gamma_5 e \left[f_{Vu} \bar{u} \gamma^\mu u + f_{Vd} \bar{d} \gamma^\mu d \right].
\end{aligned} \tag{4.28}$$

Here f_{xy} are effective couplings to be derived below for the different models.

The Lagrangian involves the product of the Z and Z' axial vector currents of the electron with the vector neutral currents of the quarks. Remembering that the

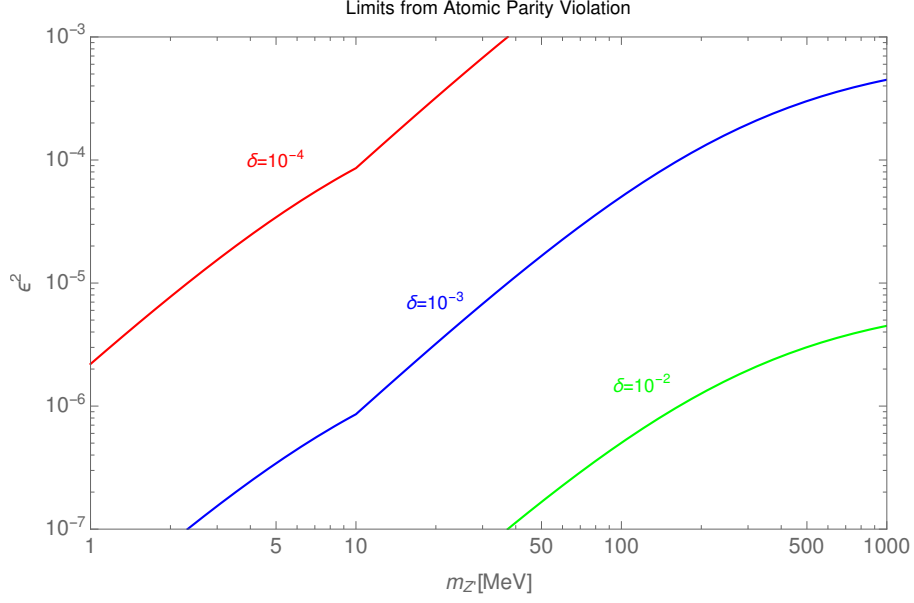


Figure 6: Upper limits on the kinetic mixing as a function of the Z' mass for different values of the mass mixing parameter δ according to the first line of Table 6.

vector part of the Z weak neutral current is associated with the Z weak charge, we get from Eq. (4.28)

$$\begin{aligned} Q_Z &= (2Z + N) \left(\frac{1}{4} - \frac{2}{3} \sin^2 \theta_W \right) + (Z + 2N) \left(-\frac{1}{4} + \frac{1}{3} \sin^2 \theta_W \right), \quad (4.29) \\ &= \frac{1}{4} [Z(1 - 4 \sin^2 \theta_W) - N] = \frac{1}{4} Q_W^{\text{SM}}(Z, N). \end{aligned}$$

The quantity Q_W^{SM} is usually referred to as weak charge of a nucleus of Z protons and N neutrons. Similarly, the quark contribution to the charge $Q_{Z'}$ associated with the vector part of the Z' current is found to be

$$Q_{Z'} = (2Z + N)f_{V_u} + (Z + 2N)f_{V_d} \quad (4.30)$$

$$= (2f_{V_u} + f_{V_d})z + (f_{V_u} + 2f_{V_d})N. \quad (4.31)$$

The effective Lagrangian Eq. (4.28) implies the following parity violation Hamiltonian density for the electron field in the vicinity of the nucleus³

$$\begin{aligned} \mathcal{H}_{\text{eff}} &= e^\dagger(\vec{r}) \gamma_5 e(\vec{r}) \left[\frac{g^2 + g'^2}{4 m_Z^2} \frac{1}{4} Q_W^{\text{SM}} - \frac{g^2 + g'^2}{4 m_{Z'}^2} \epsilon_Z^2 \left(1 - \frac{l - e}{Q_{x1} \cos_\beta^2 + Q_{x2} \sin_\beta^2} \right) Q_{Z'} \right] \delta(\vec{r}) \\ &= e^\dagger(\vec{r}) \gamma_5 e(\vec{r}) \frac{G_F}{2\sqrt{2}} Q_W^{\text{eff}}(Z, N) \delta(\vec{r}), \end{aligned} \quad (4.32)$$

³ $\delta(\vec{r})$ can be replaced by the nuclear density $\rho(\vec{r})$ to take into account finite size effects of the nucleus. For a more detailed discussion about APV see reference [78].

where

$$Q_W^{\text{eff}} = Q_W^{\text{SM}} - 4\delta^2 Q_{Z'} \left(1 - \frac{l - e}{Q_{x1} \cos^2 \beta + Q_{x2} \sin^2 \beta} \right), \quad (4.33)$$

using that $\epsilon_Z = \frac{M_{Z'}}{M_Z} \delta$. We remind the reader that l and e are the charges of the left-handed and right-handed electron under $U(1)_X$.

Notice that the effective weak charge of the nucleus Q_W^{eff} includes in addition to the standard contribution Q_W^{SM} an additional Z' contribution. In order to know Q_W^{eff} , it is necessary to calculate $Q_{Z'}$. To do so, we need to specify from Eq. (3.27) f_{V_u} and f_{V_d} associated to the Z' boson,

$$f_{V_u} = \left[\frac{1}{4} - \frac{2}{3} \sin^2 \theta_W \left(1 - \frac{\epsilon \cos \theta_W}{\epsilon_Z \sin \theta_W} \right) + \frac{1}{4} \frac{q + u}{Q_{x1} \cos^2 \beta + Q_{x2} \sin^2 \beta} \right], \quad (4.34)$$

$$f_{V_d} = \left[-\frac{1}{4} + \frac{1}{3} \sin^2 \theta_W \left(1 - \frac{\epsilon \cos \theta_W}{\epsilon_Z \sin \theta_W} \right) + \frac{1}{4} \frac{q + d}{Q_{x1} \cos^2 \beta + Q_{x2} \sin^2 \beta} \right], \quad (4.35)$$

where $q(u)$ is the charge of the left-handed (right-handed) quark field under $U(1)_X$.

Substituting (4.34) and (4.35) into (4.33) we obtain the following general expression for $\Delta Q_W = Q_W^{\text{eff}} - Q_W^{\text{SM}}$,

$$\begin{aligned} \Delta Q_W = & -\delta^2 Q_W^{\text{SM}} - \delta^2 4Z \sin \theta_W \cos \theta_W \frac{\epsilon}{\epsilon_Z} - \delta^2 \frac{(q + u)(2Z + N)}{Q_{x1} \cos^2 \beta + Q_{x2} \sin^2 \beta} \\ & - \delta^2 \frac{(q + d)(Z + 2N)}{Q_{x1} \cos^2 \beta + Q_{x2} \sin^2 \beta} \left(1 - \frac{l - e}{Q_{x1} \cos^2 \beta + Q_{x2} \sin^2 \beta} \right). \end{aligned} \quad (4.36)$$

Currently, the SM prediction for the weak nuclear charge in the Cesium case is [79]

$$Q_W^{\text{SM}} = -73.16(5), \quad (4.37)$$

so that the general expression Eq. (4.36) becomes:

$$\begin{aligned} \Delta Q_W = & 73.16\delta^2 - 220\delta \left(\epsilon \frac{M_Z}{m_{Z'}} \right) \sin \theta_W \cos \theta_W - \delta^2 \frac{188(q + u)}{Q_{x1} \cos^2 \beta + Q_{x2} \sin^2 \beta} \\ & - \delta^2 \frac{211(q + d)}{Q_{x1} \cos^2 \beta + Q_{x2} \sin^2 \beta} \left(1 - \frac{l - e}{Q_{x1} \cos^2 \beta + Q_{x2} \sin^2 \beta} \right). \end{aligned} \quad (4.38)$$

On the other hand the experimental value for the weak nuclear charge in the Cesium case is [80, 81]

$$Q_W^{\text{exp}} = -73.16(35), \quad (4.39)$$

and the 90% CL bound on the difference is [37]

$$|\Delta Q_W(Cs)| = |Q_W^{\text{exp}} - Q_W^{\text{SM}}| < 0.6, \quad (4.40)$$

which yields the general APV expression for $U(1)_X$ models for the Cesium nucleus:

$$\left| 73.16\delta^2 - 220\delta \left(\epsilon \frac{M_Z}{m'_Z} \right) \sin \theta_W \cos \theta_W - \delta^2 \frac{188(q+u)}{Q_{x1} \cos^2 \beta + Q_{x2} \sin^2 \beta} \right. \\ \left. - \delta^2 \frac{211(q+d)}{Q_{x1} \cos^2 \beta + Q_{x2} \sin^2 \beta} \left(1 - \frac{l-e}{Q_{x1} \cos^2 \beta + Q_{x2} \sin^2 \beta} \right) \right| \times K(Cs) < 0.6. \quad (4.41)$$

The correction factor $K(Cs)$ is introduced for low values of $M_{Z'}$ where the local limit approximation is not valid. Different values for this correction factor are listed in Table I of reference [78]. At first order, one can drop the terms proportional to δ^2 in Eq. (4.41) and then solve it for ϵ in terms of δ , using $220\delta \left(\epsilon \frac{M_Z}{m'_Z} \right) \sin \theta_W \cos \theta_W = 0.6$.

Doing so, we find the bound shown in the first line of Table 6. The numerical upper limit on the kinetic mixing as a function of the Z' mass for different values of δ taking into account the energy dependence on $K(Cs)$ is displayed in Fig. 6.

It is useful again to apply our procedure to a well known model in the literature such as the $B-L$ model. In this case $q = u = d = 1/3$, $Q_{x2} = 0$, $Q_{x1} = 2$, $l = e$. With these values the expression (4.38) becomes

$$\Delta Q_W = -59.84\delta^2 - 220\delta \left(\epsilon \frac{M_Z}{m'_Z} \right) \sin \theta_W \cos \theta_W - 133\delta^2 \tan^2 \beta, \quad (4.42)$$

which coincides with the expressions obtained in [37, 38], except for the last term, that arises due to the non-zero $U(1)_{B-L}$ charges of the fermions. Applying the 90% CL bound in Eq. (4.41) we get

$$\left| -59.84\delta^2 - 220\delta \left(\epsilon \frac{M_Z}{m'_Z} \right) \sin \theta_W \cos \theta_W - 133\delta^2 \tan^2 \beta \right| \times K(Cs) < 0.6. \quad (4.43)$$

From Eq. (4.43) we can see the term proportional to δ^2 can not always be dropped as we did before to obtain the limit in the first line of Table 6. For sufficiently large $\tan \beta$ the last term in Eq. (4.43) might become relevant yielding changes for the upper limits on the kinetic mixing. Since the importance of this last term is rather model dependent we will not devote time to discuss its impact here.

Regardless, the conclusion that Cesium nucleus provides an interesting and orthogonal test for new physics stands, and depending on the $U(1)_X$ model under study it gives rise to restrictive limits on the kinetic mixing parameter following Table 6.

Another observable in APV experiments is given by the value of $\sin\theta_W$ that is measured at low energies. The shift in $\sin^2\theta_W$ caused by the presence of a new vector boson that mixes with the Z boson is found to be [37]

$$\Delta\sin^2\theta_W = -0.42\epsilon\delta\frac{m_Z}{m_{Z'}}\frac{m_{Z'}^2}{m_{Z'}^2 + Q^2}, \quad (4.44)$$

where Q is the energy at which $\sin\theta_W$ is measured and $\Delta\sin^2\theta_W$ refers to the error on the measurement of $\sin^2\theta_W$ as shown in Table 6. By plugging the experimental error bar as displayed in the third column of Table 6 into Eq. (4.44) one can derive upper limits on ϵ as a function of δ as shown in the fourth column of Table 6. The first two rows in Table 6 refer to past experiments, whereas the remaining rows represent projected experimental sensitivities.

Anyways, one can see that the Qweak experiment is not expected to be as sensitive to the kinetic mixing as the first measurements, but both Moller and MESA experiments should be able to surpass previous experiments yielding tight bounds on the kinetic mixing [82–84].

4.6 Muon Anomalous Magnetic Moment

Any charged particle has a magnetic dipole moment ($\vec{\mu}$) defined as

$$\vec{\mu} = g\left(\frac{q}{2m}\right)\vec{s}, \quad (4.45)$$

where s is the spin of the particle, g is the gyromagnetic ratio, $q = \pm e$ is the electric charge of a given charged particle, and m its mass (see [16] for a recent and extensive review). Loop corrections induce deviations from the tree-level value $g = 2$, which are parametrized for the muon in terms of $a_\mu = (g_\mu - 2)/2$, referred to as the anomalous magnetic moment. An enormous effort has been dedicated to precisely determine the SM contribution to $g - 2$ [85–87]. Interestingly, the SM prediction does not agree with recent measurements leading to [88]

$$\Delta a_\mu = a_\mu^{exp} - a_\mu^{SM} = (287 \pm 80) \times 10^{-11}, \quad (4.46)$$

which implies a 3.6σ evidence for new physics. Therefore, it is definitely worthwhile to explore new physics models capable of giving rise to a positive contribution to $g - 2$. In the $U(1)_X$ models under investigation, a particle that fulfills this role is the massive Z' that yields [16, 89, 90]

$$\Delta a_\mu(f, Z') = \frac{1}{8\pi^2}\frac{m_\mu^2}{m_{Z'}^2}\int_0^1 dx \sum_f \frac{|g_v^{f\mu}|^2 F^+(x) + |g_a^{f\mu}|^2 F^-(x)}{(1-x)(1-\lambda^2 x) + \epsilon_f^2 \lambda^2 x}, \quad (4.47a)$$

with

$$F^\pm = 2x(1-x)(x-2 \pm 2\epsilon_f) + \lambda^2 x^2 (1 \mp \epsilon_f)^2 (1-x \pm \epsilon_f) \quad (4.47b)$$

and $\epsilon_f \equiv \frac{m_f}{m_\mu}$, $\lambda \equiv \frac{m_\mu}{m_{Z'}}$. Here f are charged leptons. Since we are not dealing with flavor changing interactions in this work, $\epsilon_f \equiv 1$ and $m_f = m_\mu$. Moreover, in the limit of a Z' much heavier than the muon, the contribution simplifies to

$$\Delta a_\mu(Z') \simeq \frac{1}{12\pi^2} \frac{m_\mu^2}{m_{Z'}^2} (g_v^2 - 5g_a^2), \quad (4.48)$$

where g_v and g_a are the vector and axial vector couplings of the Z' with the muon. Notice that only models where the vector coupling is more than five times larger than the axial vector couplings are capable of addressing the $g-2$ anomaly in agreement with [91]. This condition is satisfied only in the $U(1)_D$ and $U(1)_F$ models.

That said, the region that explain the $g-2$ anomaly is easily obtained through the equality

$$\frac{g_v^2}{(m_{Z'}[\text{GeV}])^2} \simeq 3.3 \times 10^{-5}. \quad (4.49)$$

For instance, in the $U(1)_D$ model $g_v = -1.75g_X$. Keeping $g_X = 1$, we need $m_{Z'} \sim 540$ GeV to accommodate the $g-2$ anomaly, which is way beyond the region of interest in this work. Anyways, such heavy gauge bosons are subject to stringent limits from dimuon searches as shown in [92–101], preventing such gauge bosons to be a solution to the $g-2$ anomaly. However, if we set $g_X = 10^{-4}$, then $m_{Z'} \sim 54$ MeV is required, being potentially able to explain the $g-2$ anomaly, as long as the kinetic and mass mixing parameters are kept sufficiently small. A more thorough discussion of the possibility of explaining $g-2$ in each of these models will be made elsewhere. It is interesting to see though, that one might be able to cure 2HDM from flavor changing interactions, generate neutrino masses, while solving a relevant and long standing anomaly in particle physics. junior

4.7 Neutrino-Electron Scattering

Intensity frontier constitutes a promising endeavor in the quest for new physics, being able to explore models inaccessible at high-energy frontiers. One canonical example are the precise measurements on neutrino-electron scattering using different targets, as measured by several experiments such as TEXONO, GEMMA, BOREXINO, LSND and CHARM. Since neutrino interactions are purely leptonic, they are subject to small uncertainties. Moreover, interesting models such as the dark photon and light Z' models such as ours, predict different signals at these experiments. Therefore, the use of neutrino-electron scattering to explore hints of new physics is both theoretically and experimentally well motivated.

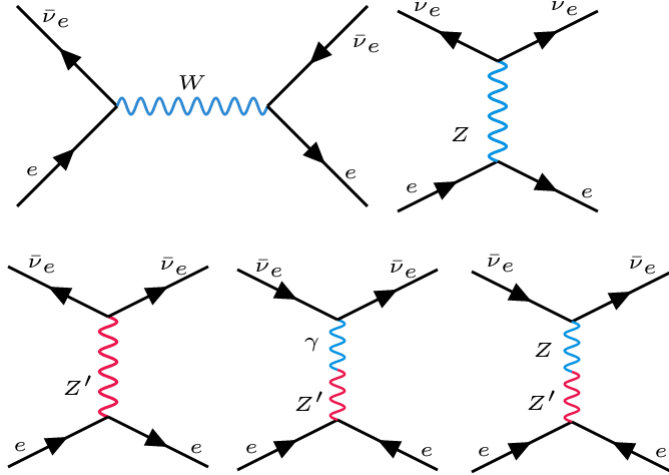


Figure 7: Feynmann diagrams relevant for neutrino-electron scattering

That said, several works have been done to place limits on new physics models based on neutrino-electron scattering data [102–107]. Here we will briefly review the concept behind these and derive constraints the gauge couplings as a function of the Z' mass.

The physics behind these constraints lies on the computation of the neutrino-electron scattering due to new physics. In Fig. 7 we exhibit the SM diagram alongside the new physics ones. Following Ref. [108] the new physics neutrino-electron scattering cross section can be parametrized in terms of the $B-L$ model which is found to be [105]

$$\frac{d\sigma}{dE_R} = \frac{g_{B-L}^4 m_e}{4\pi E_\nu^2 (m_{Z'}^2 + 2m_e E_R)^2} (2E_\nu^2 + E_R^2 - eE_R E_\nu - m_e E_R) \quad (4.50)$$

where E_R is the electron recoil energy, E_ν is the energy of the incoming neutrino, m_e is the electron mass, and G_F the Fermi constant.

The idea is to compute the expected neutrino-scattering rate from new physics, $(dR/dE_R)_{NP}$, which is related to the neutrino-electron scattering through

$$\left(\frac{dR}{dE_R} \right)_{NP} = t \rho_e \int_{E_\nu^{min}}^{\infty} \frac{d\Phi}{dE_\nu} \frac{d\sigma}{dE_R} dE_\nu, \quad (4.51)$$

where Φ is the neutrino flux, t is period of mock data taking, and ρ_e is electron number density per kg of the target mass. Once that has been computed, one compares it with the measured rate and finds 90% level limits applying a χ^2 statistics as follows:

$$\chi^2 = \sum_{i=1} \frac{(R_{\text{exp}i} - (R_{\text{SM}i} + R_{\text{NP}}))^2}{\sigma_i} \quad (4.52)$$

Table 7: Summary of experiments that constrained $\nu - e$ scattering.

Experiment	Type of neutrino	$\langle E_\nu \rangle$	T
TEXONO-NPCGe [110]	$\bar{\nu}_e$	1–2 MeV	0.35–12 keV
TEXONO-HPGe [111, 112]	$\bar{\nu}_e$	1–2 MeV	12–60 keV
TEXONO-CsI(Tl) [113]	$\bar{\nu}_e$	1–2 MeV	3–8 MeV
LSND [114]	ν_e	36 MeV	18–50 MeV
BOREXINO [115]	ν_e	862 keV	270–665 keV
GEMMA [116]	$\bar{\nu}_e$	1–2 MeV	3–25 keV
CHARM II [117]	ν_μ	23.7 GeV	3–24 GeV
CHARM II [117]	$\bar{\nu}_\mu$	19.1 GeV	3–24 GeV

where R_{exp} , R_{SM} are the measured and SM predicted rates respectively, and σ_i is the statistical error on the measurement of R_{exp} . The index i runs through energy bins. Using data from several experiments subject to different energy threshold and type of incoming neutrino flavor as summarized in Table 7, constraints on the new physics have been placed [108]. The limits were interpreted in terms of the $B - L$ model, as shown in Fig. 8. These bounds are the most restrictive for $m_{Z'} \sim 100 \text{ MeV} - 1 \text{ GeV}$, as exhibited in Fig. 9 where all relevant constraints are put together. See [109] for a recent review on neutrino-electron scattering experiments.

One needs to apply these constraints to the $U(1)_X$ models under study with care. Obviously, for the $B - L$ model in Table 2, the limits in Fig. 9 are directly applicable. For the remaining $U(1)_X$ models, one can estimate the limits through rescaling. Since the kinetic and mass-mixing are constrained to be small, the leading diagram is the t -channel Z' exchange in Fig. 7. Therefore, the scattering cross section scales with $g_{Z'-\nu-\nu}^2 g_{Z'-e-e}^2$, where $g_{Z'-\nu-\nu}$, $g_{Z'-e-e}$ are the Z' vectorial couplings with the neutrinos and electrons respectively. These are easily obtained knowing that the vector coupling with a given fermion field is $g_{fv} = g_X/2(Q_{fL} + Q_{fR})$, where Q_{fL} and Q_{fR} are the charges of the left-handed and right-handed field components under $U(1)_X$ as displayed in Table 2. In summary, there is a plot similar to Fig. 8 for each $U(1)_X$ model in this work. Clearly this exercise is outside the scope of this work. Anyways, it is clear that neutrino-electron scattering provides a competitive probe for new physics and is relevant for the $U(1)_X$ models under study. These bounds can be circumvented by tuning the kinetic mixing to sufficiently small values, similarly to the dark photon model.

4.8 Low Energy Accelerators

Low energy accelerators are capable of probing new physics models out of reach of high-energy colliders. Models with light mediators, such as the dark photon model are considered a benchmark [118, 119]. The sensitivity of low energy accelerators is

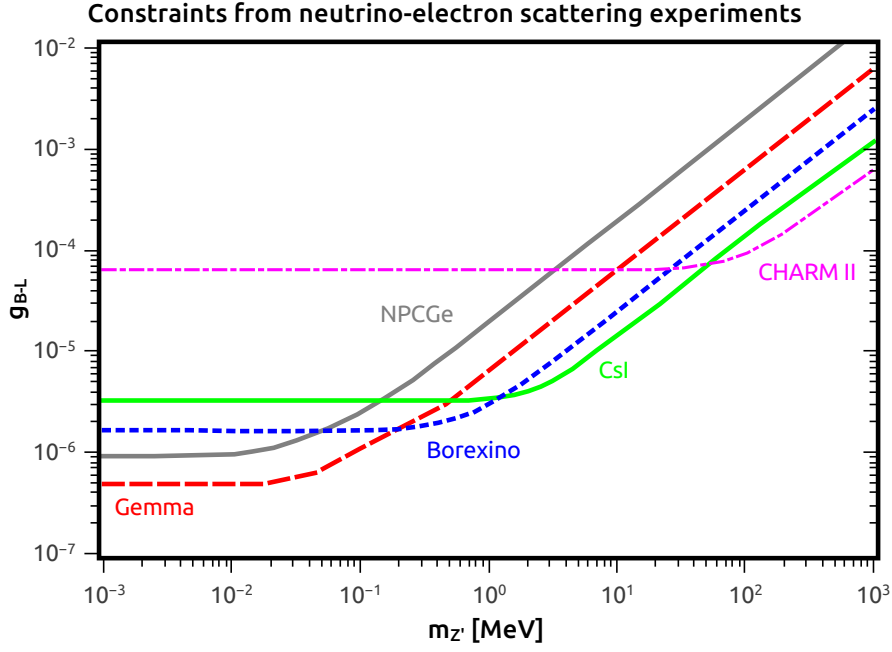


Figure 8: Constraints on the $B - L$ model based on measurements of neutrino-electron scattering.

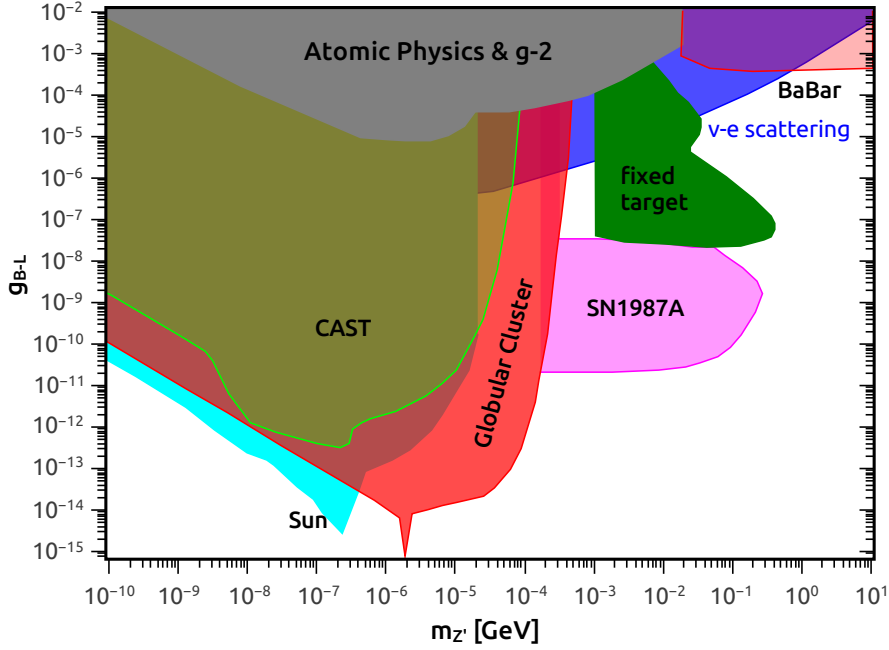


Figure 9: Summary of constraints from neutrino-electron scattering on $U(1)_X$ models with very light Z' gauge bosons. These constraints have been interpreted from dark photon searches.

driven by high-intensity beams and/or high precision detectors. Such accelerators are usually divided into two classes: (i) collider; (ii) fixed-target experiments. In the former, high-intensity beams of e^+e^- are capable of directly producing on-shell light mediators, whereas in the latter, light particles are produced as result of a decay chain created after the beam hits the target. In either case, the low-energy accelerators are excellent laboratories to spot new physics effects. In Fig. 10 we present a summary of current constraints on the dark photon model, with the dark photon, A' , decaying into charged leptons. With care, the limits exhibited in Fig. 10 can be applicable to the $U(1)_X$ investigation. For instance, the BaBar experiment searched for the $e^+e^- \rightarrow \gamma A'$, with A' decaying into l^+l^- . The interaction of the dark photon with charged leptons reads $\epsilon \bar{l} \gamma_\mu l A'^\mu$. Having in mind that the two important quantities are the production cross section and the branching ratio into electrons, one can recast the BaBar upper limits on the dark photon kinetic mixing (ϵ_{DP}) to other $U(1)_X$ models as follows

$$\epsilon_{\text{DP}}^2 \rightarrow (g_v^l)^2 BR(Z' \rightarrow l^+l^-), \quad (4.53)$$

where $g_v^l = g_X/2(Q_L^l + Q_R^l)$ is the Z' vectorial coupling to charged leptons. Here Q_L^l and Q_R^l are the left-handed and right-handed charged lepton charges under $U(1)_X$.

In all $U(1)_X$ models that accommodate neutrino masses and are free from flavor changing interactions the Z' boson features a vectorial coupling with electrons. Since the SM fermions are charged under $U(1)_X$, in addition to the kinetic mixing term, a vectorial interaction proportional to g_X also arises. Therefore, Eq. (4.53) is valid when the term proportional to g_X is dominant, otherwise, the bounds in Fig. 10 are directly applicable. Hence, one can use Eq. (4.53) to obtain limits for each $U(1)_X$ model. A similar reasoning can be applied to other collider experiments.

As for fixed target experiments such as NA48/2, the rescaling is restricted to the branching ratio into charged leptons. Sometimes these experiments include both e^+e^- and $\mu^+\mu^-$ decay modes in the analysis, while other times they consider only one of those. Our goal here is not to describe each one of these searches individually but rather present to the reader the existence of limits on the kinetic-mixing stemming from low energy accelerators. The precise bound on ϵ for each $U(1)_X$ model is not relevant for us, since they can all be evaded by simply tuning down the free kinetic mixing parameter.

Furthermore, it is worth pointing out that there is also a similar plot considering only invisible decays of the dark photon. However, as far as the $U(1)_X$ models go, the only possible invisible decay modes are the active neutrinos and right-handed neutrinos. Except in the case of the $U(1)_{B-L}$ model, this branching ratio is expected to be small, substantially weakening the limits on ϵ . Thus the searches for visible

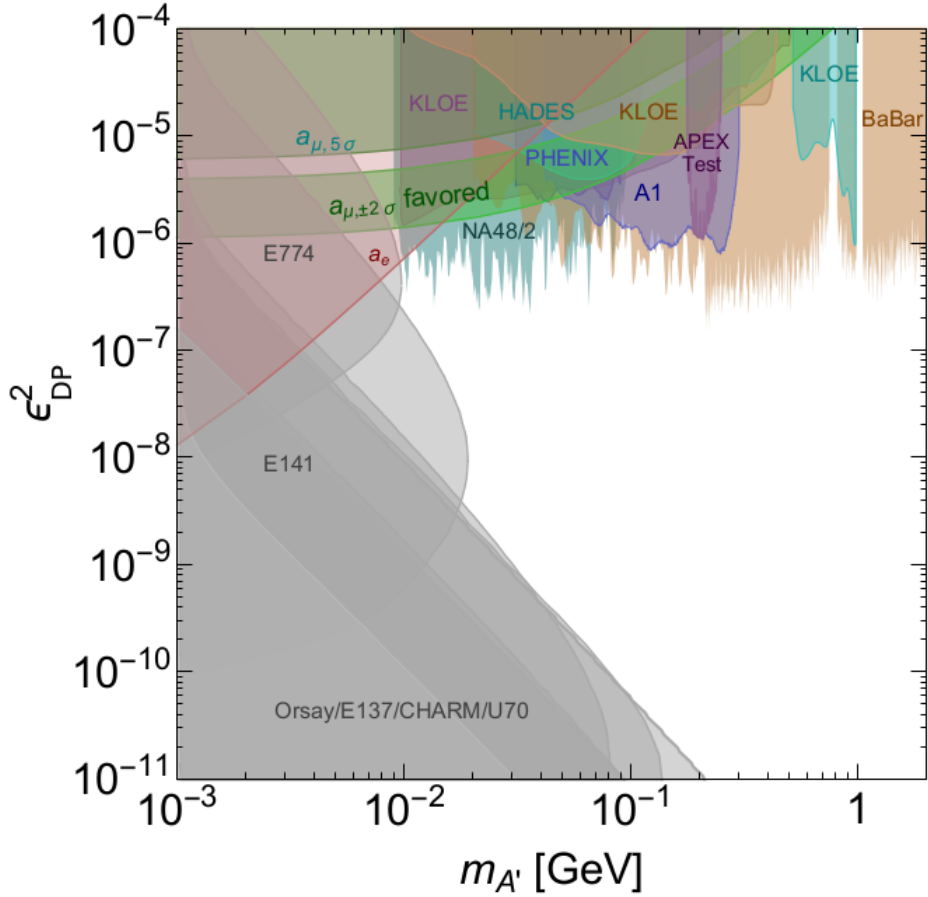


Figure 10: Summary of bounds from low energy accelerators constraints on the dark photon model [109]. After proper rescaling these constraints are also applicable to the $U(1)_X$ models in this work. In particular, the BaBar limits can be recast using the relation $\epsilon_{\text{DP}}^2 \rightarrow (g_v^l)^2 BR(Z' \rightarrow l^+l^-)$. See text for details.

decays are more constraining.

In summary, low energy accelerators yield very strong limits on the kinetic mixing parameter of the $U(1)_X$ models.

4.9 Discussion

We have discussed a variety of limits on the parameters δ and the kinetic mixing ϵ . They are model dependent. The bounds on δ were derived under the assumption that the fermions were uncharged under $U(1)_X$, where only the mass-mixing would dictate the Z' interactions with fermions. However, due to the presence of new interactions between the SM fermions and the Z' gauge boson these limits might be subject to changes by a factor of few depending on the value of g_X and fermion charges under $U(1)_X$. As for the limits on the kinetic mixing, they were obtained assuming that

the kinetic mixing alone dictates the observables since they were originally meant for the dark photon model. Since both δ and ϵ , in principle, are arbitrarily small, the constraints presented in this work might be circumvented. A more detailed analysis incorporating precise bounds on the $U(1)_X$ models is left for the future. The goal of this work was to propose new 2HDM gauge models capable of accommodating neutrino masses and freeing the 2HDM from flavor changing interactions, as well as estimate what kind of phenomenology these models can generate.

On a side note, one more interesting avenue that is worth exploring is the near future is the possibility of accommodating a dark matter candidate. Naively, one could have a Sub-GeV singlet fermion charged under $U(1)_X$ that interacts with SM fermions through the light Z' gauge boson, scenario which has been studied before in different contexts [120–124].

5 Conclusions

Two Higgs Doublet Models are a natural extension of the Standard Model with interesting Higgs and collider phenomenology. These models are plagued with flavor changing interactions and for this reason a Z_2 symmetry has in the past been evoked to save such flavor changing couplings from tight flavor constraints. In this work, we cure 2HDM model flavor changing interactions from gauge principles and additionally embed neutrino neutrino masses via the see-saw mechanism. In particular, we propose eight different models where neutrino masses and absence of flavor changing interactions are nicely explained. To do so, we gauge an Abelian gauge group that gives rise to a massive Z' via spontaneous symmetry breaking. We work in the light Z' regime, $m_{Z'} \ll m_Z$, and investigate the associated phenomenology touching rare meson decays, Higgs physics, LEP precision data, neutrino-electron scattering, low energy accelerators and LHC probes.

In summary, we find that these models give rise to a rather rich phenomenology and can be made compatible with data while successfully generating neutrino masses and freeing 2HDM from flavor changing interactions.

Acknowledgments

The authors are greatly thankful to Brian Batell, Rouven Essig and David Morrissey for correspondence. We are specially thankful to Rouven for providing the data files needed for Fig.10. FSQ is grateful to Carlos Pires, Paulo Rodrigues and Alvaro Ferraz for their hospitality at UFPB and UFRN where this project was partially conducted. FSQ thanks Fabio Iocco, Enrico Bertuzzo and Manuela Vecchi for the great Dark Matter Workshop in Sao Paulo where this project was finalized. D.C thanks João

Silva and Jorge Romão from the CFTP Lisbon for useful discussions, time and motivation to develop this work. DC is partly supported by the Brazilian National Council for Scientific and Technological Development (CNPq), under grants 484157/2013-2 and 201066/2015-7. TM is supported by Coordenação de Aperfeiçoamento de Pessoal de Nível Superior (Capes). WR is supported by the DFG with grant RO 2516/6-1 in the Heisenberg Programme. M.C was supported by the IMPRS-PTFS.

A Conditions for Anomaly Freedom

Generically we will call the $U(1)_X$ charges Y' , where $Y' = l, q, e, u, d$. The anomaly free conditions can be read as:

$[SU(3)_c]^2 U(1)_X$:

$$\begin{aligned} \mathcal{A} &= \text{Tr} \left[\left\{ \frac{\lambda^a}{2}, \frac{\lambda^b}{2} \right\} Y'_R \right] - \text{Tr} \left[\left\{ \frac{\lambda^a}{2}, \frac{\lambda^b}{2} \right\} Y'_L \right] \\ \mathcal{A} &\propto \sum_{\text{quarks}} Y'_R - \sum_{\text{quarks}} Y'_L = [3u + 3d] - [3 \cdot 2q] = 0. \end{aligned}$$

Therefore,

$$u + d - 2q = 0. \quad (\text{A.1})$$

$[SU(2)_L]^2 U(1)_X$:

$$\mathcal{A} = -\text{Tr} \left[\left\{ \frac{\sigma^a}{2}, \frac{\sigma^b}{2} \right\} Y'_L \right] \propto -\sum Y_L = -[2l + 3 \cdot 2q] = 0.$$

Therefore,

$$l = -3q. \quad (\text{A.2})$$

$[U(1)_Y]^2 U(1)_X$:

$$\begin{aligned} \mathcal{A} &= \text{Tr} [\{Y'_R, Y'_R\} Y'_R] - \text{Tr} [\{Y'_L, Y'_L\} Y'_L] \propto \sum Y_R^2 Y'_R - \sum Y_L^2 Y'_L \\ \mathcal{A} &\propto \left[(-2)^2 e + 3 \left(\frac{4}{3} \right)^2 u + 3 \left(-\frac{2}{3} \right)^2 d \right] - \left[2(-1)^2 l + 3 \cdot 2 \left(\frac{1}{3} \right)^2 q \right] = 0. \end{aligned}$$

Therefore,

$$6e + 8u + 2d - 3l - q = 0. \quad (\text{A.3})$$

$U(1)_Y [U(1)_X]^2$:

$$\begin{aligned} \mathcal{A} &= \text{Tr} [\{Y'_R, Y'_R\} Y'_R] - \text{Tr} [\{Y'_L, Y'_L\} Y'_L] \propto \sum Y_R Y_R'^2 - \sum Y_L Y_L'^2 \\ \mathcal{A} &\propto \left[(-2) e^2 + 3 \left(\frac{4}{3} \right) u^2 + 3 \left(-\frac{2}{3} \right) d^2 \right] - \left[2(-1) l^2 + 3 \cdot 2 \left(\frac{1}{3} \right) q^2 \right] = 0. \end{aligned}$$

Therefore,

$$-e^2 + 2u^2 - d^2 + l^2 - q^2 = 0. \quad (\text{A.4})$$

$[U(1)_X]^3$:

$$\begin{aligned} \mathcal{A} &= \text{Tr} [\{Y'_R, Y'_R\} Y'_R] - \text{Tr} [\{Y'_L, Y'_L\} Y'_L] \propto \sum Y'_R{}^3 - \sum Y'_L{}^3 \\ \mathcal{A} &\propto [e^3 + 3u^3 + 3d^3] - [2l^3 + 3 \cdot 2q^3] = 0. \end{aligned}$$

Therefore,

$$e^3 + 3u^3 + 3d^3 - 2l^3 - 6q^3 = 0. \quad (\text{A.5})$$

B Gauge bosons

We will now derive the physical gauge boson spectrum, first of all let us write the covariant derivative Eq. (3.19) in terms of ϵ as

$$D_\mu = \partial_\mu + igT^a W_\mu^a + ig' \frac{Q_Y}{2} B_\mu + \frac{i}{2} \left(g' \frac{\epsilon Q_Y}{\cos \theta_W} + g_X Q_X \right) X_\mu, \quad (\text{B.1})$$

or explicitly,

$$D_\mu = \partial_\mu + \frac{i}{2} \begin{pmatrix} gW_\mu^3 + g'Q_Y B_\mu + G_X X_\mu & g\sqrt{2}W_\mu^+ \\ g\sqrt{2}W_\mu^- & -gW_\mu^3 + g'Q_Y B_\mu + G_X X_\mu \end{pmatrix}, \quad (\text{B.2})$$

where we defined for simplicity

$$G_{X_i} = \frac{g'\epsilon Q_{Y_i}}{\cos \theta_W} + g_X Q_{X_i} \quad (\text{B.3})$$

with Q_{Y_i} being the hypercharge of the scalar doublet under $SU(2)_L$, which in the 2HDM is taken to equal to +1 for both scalar doublets; Q_{X_i} is charge of the scalar doublet i under $U(1)_X$.

We will use $D_\mu \Phi_i$ to refer to the action of the covariant derivative on the i scalar doublet of $Y = 1$ ($i = 1, 2$). Disregarding the term ∂_μ we have

$$D_\mu \Phi_i = \frac{i}{2\sqrt{2}} \begin{pmatrix} gW_\mu^3 + g'B_\mu + G_{X_i} X_\mu & g\sqrt{2}W_\mu^+ \\ g\sqrt{2}W_\mu^- & -gW_\mu^3 + g'B_\mu + G_{X_i} X_\mu \end{pmatrix} \begin{pmatrix} 0 \\ v_i \end{pmatrix}, \quad (\text{B.4})$$

$$D_\mu \Phi_i = \frac{i}{2\sqrt{2}} v_i \begin{pmatrix} \sqrt{2}gW_\mu^+ \\ -gW_\mu^3 + g'B_\mu + G_{X_i} X_\mu \end{pmatrix}. \quad (\text{B.5})$$

Consequently,

$$\begin{aligned} (D_\mu \Phi_i)^\dagger (D^\mu \Phi_i) &= \frac{1}{4} v_i^2 g^2 W_\mu^- W^{+\mu} + \frac{1}{8} v_i^2 [g^2 W_\mu^3 W^{3\mu} + g'^2 B_\mu B^\mu + G_{X_i}^2 X_\mu X^\mu] \\ &\quad + \frac{1}{8} v_i^2 [-2gg'W_\mu^3 B^\mu - 2gG_{X_i}W_\mu^3 X^\mu + 2g'G_{X_i}B_\mu X^\mu]. \end{aligned} \quad (\text{B.6})$$

Carrying out the electroweak rotation as usual,

$$\begin{aligned} B_\mu &= \cos \theta_W A_\mu - \sin \theta_W Z_\mu^0 \\ W_\mu^3 &= \sin \theta_W A_\mu + \cos \theta_W Z_\mu^0, \end{aligned} \quad (\text{B.7})$$

we obtain

$$(D_\mu \Phi_i)^\dagger (D^\mu \Phi_i) = \frac{1}{4} v_i^2 g^2 W_\mu^- W^{+\mu} + \frac{1}{8} v_i^2 [g_Z^2 Z_\mu^0 Z^{0\mu} + G_{X_i}^2 X_\mu X^\mu - 2g_Z G_{X_i} Z_\mu^0 X^\mu], \quad (\text{B.8})$$

where $g_Z^2 = g^2 + g'^2 = g^2 / \cos^2 \theta_W$. As we can see, after the rotation Eq. (B.7) the field A_μ identified as the photon is massless, as it must be.

For the singlet Φ_S (with $Q_Y = 0$ and $T^a = 0$ and disregarding the ∂_μ term) we obtain

$$D_\mu \Phi_S = \frac{i}{2\sqrt{2}} v_s g_X q_X X_\mu, \quad (\text{B.9})$$

so that

$$(D_\mu \Phi_S)^\dagger (D^\mu \Phi_S) = \frac{1}{8} v_s^2 g_X^2 q_X^2 X_\mu X^\mu. \quad (\text{B.10})$$

Notice from Eq. (B.10) that the singlet only contributes to the $U(1)_X$ gauge boson mass. Then:

$$\begin{aligned} \mathcal{L}_{\text{mass}} &= (D_\mu \Phi_1)^\dagger (D^\mu \Phi_1) + (D_\mu \Phi_2)^\dagger (D^\mu \Phi_2) + (D_\mu \Phi_S)^\dagger (D^\mu \Phi_S) \\ &= \frac{1}{4} g^2 v^2 W_\mu^- W^{+\mu} + \frac{1}{8} g_Z^2 v^2 Z_\mu^0 Z^{0\mu} - \frac{1}{4} g_Z (G_{X1} v_1^2 + G_{X2} v_2^2) Z_\mu^0 X^\mu \\ &\quad + \frac{1}{8} (v_1^2 G_{X1}^2 + v_2^2 G_{X2}^2 + v_s^2 g_X^2 q_X^2) X_\mu X^\mu, \end{aligned} \quad (\text{B.11})$$

where $v^2 = v_1^2 + v_2^2$. Finally Eq. (B.11) can be written as

$$\mathcal{L}_{\text{mass}} = m_W^2 W_\mu^- W^{+\mu} + \frac{1}{2} m_{Z^0}^2 Z_\mu^0 Z^{0\mu} - \Delta^2 Z_\mu^0 X^\mu + \frac{1}{2} m_X^2 X_\mu X^\mu, \quad (\text{B.12})$$

where

$$m_W^2 = \frac{1}{4} g^2 v^2, \quad (\text{B.13})$$

$$m_{Z^0}^2 = \frac{1}{4} g_Z^2 v^2, \quad (\text{B.14})$$

$$\Delta^2 = \frac{1}{4} g_Z (G_{X1} v_1^2 + G_{X2} v_2^2), \quad (\text{B.15})$$

$$m_X^2 = \frac{1}{4} (v_1^2 G_{X1}^2 + v_2^2 G_{X2}^2 + v_s^2 g_X^2 q_X^2). \quad (\text{B.16})$$

Summarizing, after the symmetry breaking pattern of this model we realize that there is a remaining mixing between Z_μ^0 and X_μ , that may be expressed through the matrix

$$m_{Z^0 X}^2 = \frac{1}{2} \begin{pmatrix} m_{Z^0}^2 & -\Delta^2 \\ -\Delta^2 & m_X^2 \end{pmatrix}, \quad (\text{B.17})$$

or explicitly

$$m_{Z^0 X}^2 = \frac{1}{8} \begin{pmatrix} g_Z^2 v^2 & -g_Z (G_{X1} v_1^2 + G_{X2} v_2^2) \\ -g_Z (G_{X1} v_1^2 + G_{X2} v_2^2) & v_1^2 G_{X1}^2 + v_2^2 G_{X2}^2 + v_s^2 g_X^2 q_X^2 \end{pmatrix} \quad (\text{B.18})$$

The above expression Eq. (B.18) for the mixing between the Z_μ^0 and X_μ bosons is given as function of arbitrary $U(1)_X$ charges of doublets/singlet scalars. It is important to note that when $Q_{X1} = Q_{X2}$, and there is not singlet contribution, the determinant of the matrix Eq.(B.18) is zero.

Eq. (B.18) is diagonalized through a rotation $O(\xi)$

$$\begin{pmatrix} Z_\mu \\ Z'_\mu \end{pmatrix} = \begin{pmatrix} \cos \xi & -\sin \xi \\ \sin \xi & \cos \xi \end{pmatrix} \begin{pmatrix} Z_\mu^0 \\ X_\mu \end{pmatrix}, \quad (\text{B.19})$$

and its eigenvalues are:

$$\begin{aligned} m_Z^2 &= \frac{1}{2} \left[m_{Z^0}^2 + m_X^2 + \sqrt{(m_{Z^0}^2 - m_X^2)^2 + 4(\Delta^2)^2} \right] \\ m_{Z'}^2 &= \frac{1}{2} \left[m_{Z^0}^2 + m_X^2 - \sqrt{(m_{Z^0}^2 - m_X^2)^2 + 4(\Delta^2)^2} \right]. \end{aligned} \quad (\text{B.20})$$

The ξ angle is given by

$$\tan 2\xi = \frac{2\Delta^2}{m_{Z^0}^2 - m_X^2}. \quad (\text{B.21})$$

The expressions for the gauge boson masses above are general but not very intuitive. We will simplify these equations by working in the limit in which the mass mixing is small and the Z' is much lighter than the Z boson. That said, we can find a reduced formula for the masses as follows

$$m_Z^2 \simeq \frac{1}{2} \left[m_{Z^0}^2 + \sqrt{m_{Z^0}^4 + 4(\Delta^2)^2} \right] \simeq \frac{1}{2} [m_{Z^0}^2 + m_{Z^0}^2].$$

In this case:

$$m_Z^2 \simeq m_{Z^0}^2 = \frac{1}{4} g_Z^2 v^2, \quad (\text{B.22})$$

being $g_Z = \frac{g}{\cos \theta_W}$. Similarly for the Z' one finds

$$\begin{aligned} m_{Z'}^2 &= \frac{1}{2} \left[m_{Z^0}^2 + m_X^2 - \sqrt{(m_{Z^0}^2 - m_X^2)^2 + 4(\Delta^2)^2} \right] \\ &= \frac{1}{2} \left\{ m_{Z^0}^2 + m_X^2 - (m_{Z^0}^2 - m_X^2) \left[1 + \frac{4(\Delta^2)^2}{(m_{Z^0}^2 - m_X^2)^2} \right]^{\frac{1}{2}} \right\} \\ &\simeq \frac{1}{2} \left\{ m_{Z^0}^2 + m_X^2 - (m_{Z^0}^2 - m_X^2) \left[1 + \frac{2(\Delta^2)^2}{(m_{Z^0}^2 - m_X^2)^2} \right] \right\} \\ &\simeq \frac{1}{2} \left[m_{Z^0}^2 + m_X^2 - m_{Z^0}^2 + m_X^2 - \frac{2(\Delta^2)^2}{m_{Z^0}^2} \right] \\ &\simeq m_X^2 - \frac{(\Delta^2)^2}{m_{Z^0}^2}, \end{aligned} \quad (\text{B.23})$$

We may also further simplify Eq. (B.23) by working out explicitly Δ in the small-mixing regime of interest. The mixing angle must satisfy $\xi \ll 1$ by the measurements of LEP experiment, i.e.

$$\tan 2\xi \simeq \sin 2\xi \simeq 2\xi \quad (\text{B.24})$$

with which one gets

$$\xi \simeq \frac{\Delta^2}{m_{Z^0}^2 - m_X^2}. \quad (\text{B.25})$$

For the case $m_{Z^0}^2 \gg m_X^2$ we find

$$\xi \simeq \frac{\Delta^2}{m_{Z^0}^2} = \frac{1}{g_Z} (G_{X1} \cos^2 \beta + G_{X2} \sin^2 \beta). \quad (\text{B.26})$$

Substituting the Eq. (B.3) into Eq. (B.26) we obtain

$$\xi \simeq \frac{1}{g_Z} \left[\left(\frac{g' \epsilon Q_{Y1}}{\cos \theta_W} + g_X Q_{X1} \right) \cos^2 \beta + \left(\frac{g' \epsilon Q_{Y2}}{\cos \theta_W} + g_X Q_{X2} \right) \sin^2 \beta \right]. \quad (\text{B.27})$$

which simplifies to

$$\xi \simeq \frac{1}{g_Z} \left[(g_X Q_{X1} \cos^2 \beta + g_X Q_{X2} \sin^2 \beta) + \left(\frac{g' \epsilon Q_{Y1}}{\cos \theta_W} \cos^2 \beta + \frac{g' \epsilon Q_{Y2}}{\cos \theta_W} \sin^2 \beta \right) \right]. \quad (\text{B.28})$$

Since both Higgs doublets have the same hypercharge equal to +1, $g' = e/\sin \theta_W$ and $g = e/\cos \theta_W$, we further reduce Eq. (B.28) to

$$\xi \simeq \frac{\Delta^2}{m_{Z^0}^2} = \frac{g_X}{g_Z} (Q_{X1} \cos^2 \beta + Q_{X2} \sin^2 \beta) + \epsilon \tan \theta_W, \quad (\text{B.29})$$

which can also be written as

$$\xi = \epsilon_Z + \epsilon \tan \theta_W \quad (\text{B.30})$$

where

$$\epsilon_Z \equiv \frac{g_X}{g_Z} (Q_{X1} \cos^2 \beta + Q_{X2} \sin^2 \beta). \quad (\text{B.31})$$

Eq. (B.29) is the general expression for the mass-mixing between the Z boson and the Z' stemming from an arbitrary $U(1)_X$ symmetry in the limit $m_{Z'} \ll m_Z$.

In particular, for the $B - L$ case it is straightforward to prove that Eq. (B.29) becomes

$$\xi \simeq \frac{\Delta^2}{m_{Z^0}^2} \simeq 2 \frac{g_X}{g_Z} \cos^2 \beta + \epsilon \tan \theta_W = \epsilon_Z + \epsilon \tan \theta_W, \quad (\text{B.32})$$

where

$$\epsilon_Z = 2 \frac{g_X}{g_Z} \cos^2 \beta, \quad (\text{B.33})$$

in agreement with [41]. The parameter ϵ_Z appears often throughout the manuscript via its connection to the ξ in Eq. (B.29).

Anyways, with Eq. (B.29) we can obtain the general expression for the Z' mass. To do so, we need a few ingredients. Firstly, notice that

$$\begin{aligned} \frac{\Delta^4}{m_Z^2} &= \frac{g_X^2 v^2}{4} Q_{X1} \cos^2 \beta (1 - \sin^2 \beta) + \frac{g_X^2 v^2}{2} Q_{X1} Q_{X2} \cos^2 \beta \sin^2 \beta \\ &\quad + \frac{g_X^2 v^2}{4} Q_{X2}^2 \sin^2 \beta (1 - \cos^2 \beta) + \frac{g_Z^2 v^2 \epsilon^2}{4} \tan^2 \theta_W \\ &\quad - \frac{g_X g_Z v^2}{2} (Q_{X1} \cos^2 \beta + Q_{X2} \sin^2 \beta) \epsilon \tan \theta_W, \end{aligned} \quad (\text{B.34})$$

with m_Z^2 defined in Eq. (B.14). Secondly, expanding Eq. (B.16) we get

$$m_X^2 = \frac{1}{4} [v_1^2 (g_X Q_{X1} + g_Z \epsilon \tan \theta_W Q_{Y1})^2 + v_2^2 (g_X Q_{X2} + g_Z \epsilon \tan \theta_W Q_{Y2})^2 + v_s^2 g_X^2 q_X^2] \quad (\text{B.35})$$

which simplifies to

$$\begin{aligned} m_X^2 &= \frac{g_Z^2 \epsilon^2 \tan^2 \theta_W v^2}{4} + \frac{g_X^2}{4} (Q_{X1}^2 v_1^2 + Q_{X2}^2 v_2^2) \\ &\quad + \frac{g_X g_Z \epsilon \tan \theta_W}{2} (Q_{X1} v_1^2 + Q_{X2} v_2^2) + \frac{v_s^2 g_X^2 q_X^2}{4}. \end{aligned} \quad (\text{B.36})$$

Now substituting Eq. (B.34) and Eq. (B.36) into Eq. (B.23) we find

$$\begin{aligned} m_{Z'}^2 &= \frac{v_s^2}{4} g_X^2 q_X^2 + \frac{g_X^2 v^2}{4} Q_{X1}^2 \sin^2 \beta \cos^2 \beta + \frac{g_X^2 v^2}{4} Q_{X2}^2 \cos^2 \beta \sin^2 \beta \\ &\quad - \frac{g_X^2 v^2}{2} Q_{X1} Q_{X2} \cos^2 \beta \sin^2 \beta \end{aligned} \quad (\text{B.37})$$

which reduces to

$$m_{Z'}^2 = \frac{v_s^2}{4} g_X^2 q_X^2 + \frac{g_X^2 v^2 \cos^2 \beta \sin^2 \beta}{4} (Q_{X1} - Q_{X2})^2. \quad (\text{B.38})$$

We emphasize that q_X , Q_{X1} , Q_{X2} are the charges under $U(1)_X$ of the singlet scalar, Higgs doublets Φ_1 and Φ_2 respectively, $\tan \beta = v_2/v_1$, $v = 246$ GeV, v_s sets the $U(1)_X$ scale of spontaneous symmetry breaking, and g_X is the coupling constant of the $U(1)_X$ symmetry. Eq. (B.38) accounts for the Z' mass for every single $U(1)_X$ models studied in this work.

A few remarks are in order:

- (i) The Z' mass is controlled by g_X . Thus in order to achieve $m_{Z'} \ll m_Z$ one needs to sufficiently suppress this coupling.
- (ii) The Z' mass is generated via spontaneous symmetry breaking and for this reason it depends on the v_s which sets the $U(1)_X$ breaking and v due to the $Z - Z'$ mass mixing.

(iii) The Z' mass as expected depends on the $U(1)_X$ charges of the scalar doublets and the singlet scalar since they all enter into the covariant derivative of the respective scalar field from which the Z and Z' are obtained.

(iv) If $(Q_{X1} - Q_{X2})^2$ is not much larger than four as occurs for many $U(1)_X$ models in Table 2, then $m_{Z'}$ is approximately

$$m_{Z'}^2 = \frac{v_s^2}{4} g_X^2 q_X^2. \quad (\text{B.39})$$

For instance, in the $B - L$ model, $Q_{X1} = 2, q_X = 2, Q_{X2} = 0$, implying that

$$B - L : m_{Z'}^2 = v_s^2 g_X^2 + g_X^2 v^2 \cos^2 \beta \sin^2 \beta. \quad (\text{B.40})$$

Setting $v_s = 1$ TeV, we need $g_X = 10^{-3} - 10^{-6}$ to achieve $m_{Z'} = 1$ MeV – 1 GeV. Notice that this small coupling constant is a feature common to all dark photon-like models such as ours.

C δ Parameter

Defining $\tan \beta_d = \frac{v_s}{v_1}$, we can write $m_{Z'}$ from (B.38) as:

$$\begin{aligned} m_{Z'}^2 &= \frac{g_X^2 v^2 \cos^2 \beta [\sin^2 \beta (Q_{X1} - Q_{X2})^2 + \tan^2 \beta_d q_X^2]}{4}, \\ &= \frac{g_X^2 v^2 \cos^2 \beta [q_X^2 + \cos^2 \beta_d (\sin^2 \beta (Q_{X1} - Q_{X2})^2 - q_X^2)]}{4 \cos^2 \beta_d}, \end{aligned} \quad (\text{C.1})$$

$$\begin{aligned} \Rightarrow m_{Z'} &= g_X v \cos^2 \beta \frac{\sqrt{[q_X^2 + \cos^2 \beta_d (\sin^2 \beta (Q_{X1} - Q_{X2})^2 - q_X^2)]}}{2 \cos \beta \cos \beta_d}, \\ &= \frac{g_X v \cos^2 \beta}{\delta}, \end{aligned} \quad (\text{C.2})$$

with

$$\delta = \frac{2 \cos \beta \cos \beta_d}{\sqrt{[q_X^2 + \cos^2 \beta_d (\sin^2 \beta (Q_{X1} - Q_{X2})^2 - q_X^2)]}}. \quad (\text{C.3})$$

Even in this general scenario we realize that there is a relation among the masses of the neutral gauge bosons and ϵ_Z from Eq. (B.31):

$$\delta = \frac{m_Z}{m_{Z'}} \epsilon_Z. \quad (\text{C.4})$$

In the $B - L$ model where $Q_{X1} = 2, q_X = 2, Q_{X2} = 0$, δ from Eq. (C.3) is reduced to

$$\delta = \frac{\cos \beta \cos \beta_d}{\sqrt{1 - \cos^2 \beta \cos^2 \beta_d}}, \quad (\text{C.5})$$

and Eq. (C.4) is reproduced for the $m_{Z'}$ and δ values given in equations Eq. (B.40) and Eq. (C.5), respectively. In the doublets only case, $v_s = 0$, $\cos \beta_d = 1$ and consequently (C.5) becomes

$$\delta \tan \beta = 1. \quad (\text{C.6})$$

On the other hand, in the limit $v_2 \gg v_1$ and $v_s \gg v_1$:

$$\delta \simeq \cos \beta \cos \beta_d \simeq \frac{1}{\tan \beta \tan \beta_d}. \quad (\text{C.7})$$

D Currents for Z and Z'

In this section we will derive the generalized interactions among fermions and gauge bosons from the following Lagrangian:

$$\mathcal{L}_{\text{fermion}} = \sum_{\text{fermions}} \bar{\Psi}^L i \gamma^\mu D_\mu \Psi^L + \bar{\Psi}^R i \gamma^\mu D_\mu \Psi^R. \quad (\text{D.1})$$

After the electroweak rotation (B.7) the covariant derivative Eq. (3.19) for neutral gauge bosons becomes (the charged interactions are the same as those of the SM):

$$D_\mu^L = i g T^3 (\sin \theta_W A_\mu + \cos \theta_W Z_\mu^0) + i g' \frac{Q_Y}{2} (\cos \theta_W A_\mu - \sin \theta_W Z_\mu^0) + \frac{i}{2} \left(g' Q_Y \frac{\epsilon}{\cos \theta_W} + g_X Q_X \right) X_\mu. \quad (\text{D.2})$$

In Appendix B we have demonstrated that after the final SSB process a mixing between Z_μ^0 and X_μ remains, and this is the origin of δ . Replacing Z_μ^0 and X_μ as function of the physical bosons Z_μ and Z'_μ , Eq. (B.19), we obtain

$$\begin{aligned} \bar{\Psi}^L i \gamma^\mu D_\mu^L \Psi^L &= - e Q_f \bar{\psi}_f^L \gamma^\mu \psi_f^L A_\mu \\ &\quad - \left[g_Z (T_{3f}^L - Q_f \sin^2 \theta_W) \cos \xi - \frac{1}{2} (\epsilon g_Z Q_{Yf}^L \tan \theta_W + g_X Q_{Xf}^L) \sin \xi \right] \bar{\psi}_f^L \gamma^\mu \psi_f^L Z_\mu \\ &\quad - \left[g_Z (T_{3f}^L - Q_f \sin^2 \theta_W) \sin \xi + \frac{1}{2} (\epsilon g_Z Q_{Yf}^L \tan \theta_W + g_X Q_{Xf}^L) \cos \xi \right] \bar{\psi}_f^L \gamma^\mu \psi_f^L Z'_\mu, \end{aligned} \quad (\text{D.3})$$

where the relations $g \sin \theta_W = g' \cos \theta_W = e$, $g_Z = g / \cos \theta_W$, $g' = g_Z \sin \theta_W$ and $T^3 + Q_Y/2 = Q_f$ have been used. For the right-handed fields it suffices to replace T_{3f}^L for $T_{3f}^R = 0$, in which case:

$$\begin{aligned} \bar{\Psi}^R i \gamma^\mu D_\mu^R \Psi^R &= - e Q_f \bar{\psi}_f^R \gamma^\mu \psi_f^R A_\mu \\ &\quad - \left[-g_Z Q_f \sin^2 \theta_W \cos \xi - \frac{1}{2} (\epsilon g_Z Q_{Yf}^R \tan \theta_W + g_X Q_{Xf}^R) \sin \xi \right] \bar{\psi}_f^R \gamma^\mu \psi_f^R Z_\mu \\ &\quad - \left[-g_Z Q_f \sin^2 \theta_W \sin \xi + \frac{1}{2} (\epsilon g_Z Q_{Yf}^R \tan \theta_W + g_X Q_{Xf}^R) \cos \xi \right] \bar{\psi}_f^R \gamma^\mu \psi_f^R Z'_\mu. \end{aligned} \quad (\text{D.4})$$

The generalized interactions among fermions and gauge bosons, Eq. (D.1), is the sum of the contributions (D.3) and (D.4), and can be written as follows:

$$\begin{aligned}
\mathcal{L}_{\text{fermion}} = & -eQ_f \bar{\psi}_f \gamma^\mu \psi_f A_\mu \\
& - \left[g_Z (T_{3f} - Q_f \sin^2 \theta_W) \cos \xi - \frac{1}{2} \epsilon g_Z Q_{Yf}^L \tan \theta_W \sin \xi \right] \bar{\psi}_f^L \gamma^\mu \psi_f^L Z_\mu \\
& - \left[-g_Z Q_f \sin^2 \theta_W \cos \xi - \frac{1}{2} \epsilon g_Z Q_{Yf}^R \tan \theta_W \sin \xi \right] \bar{\psi}_f^R \gamma^\mu \psi_f^R Z_\mu \\
& - \left[g_Z (T_{3f} - Q_f \sin^2 \theta_W) \sin \xi + \frac{1}{2} \epsilon g_Z Q_{Yf}^L \tan \theta_W \cos \xi \right] \bar{\psi}_f^L \gamma^\mu \psi_f^L Z'_\mu \\
& - \left[-g_Z Q_f \sin^2 \theta_W \sin \xi + \frac{1}{2} \epsilon g_Z Q_{Yf}^R \tan \theta_W \cos \xi \right] \bar{\psi}_f^R \gamma^\mu \psi_f^R Z'_\mu \\
& + \frac{1}{2} g_X Q_{Xf}^L \sin \xi \bar{\psi}_f^L \gamma^\mu \psi_f^L Z_\mu + \frac{1}{2} g_X Q_{Xf}^R \sin \xi \bar{\psi}_f^R \gamma^\mu \psi_f^R Z_\mu - \frac{1}{2} g_X Q_{Xf}^L \cos \xi \bar{\psi}_f^L \gamma^\mu \psi_f^L Z'_\mu \\
& - \frac{1}{2} g_X Q_{Xf}^R \cos \xi \bar{\psi}_f^R \gamma^\mu \psi_f^R Z'_\mu.
\end{aligned} \tag{D.5}$$

The last two lines of (D.5) are the contributions introduced when the charges of the fermions under $U(1)_X$ are non-zero. In Appendix E we derive explicitly the neutral currents of both Z and Dark Z bosons of reference [41] ($Q_X^{L,R} = 0$ case). After that Eq. (D.5) can be written as

$$\begin{aligned}
\mathcal{L} = & -eJ_{em}^\mu A_\mu - \frac{g_Z}{2} J_{NC}^\mu Z_\mu - \left(\epsilon e J_{em}^\mu + \frac{\epsilon_Z g_Z}{2} J_{NC}^\mu \right) Z'_\mu \\
& + \frac{1}{4} g_X \sin \xi \left[(Q_{Xf}^R + Q_{Xf}^L) \bar{\psi}_f \gamma^\mu \psi_f + (Q_{Xf}^R - Q_{Xf}^L) \bar{\psi}_f \gamma^\mu \gamma_5 \psi_f \right] Z_\mu \\
& - \frac{1}{4} g_X \cos \xi \left[(Q_{Xf}^R + Q_{Xf}^L) \bar{\psi}_f \gamma^\mu \psi_f - (Q_{Xf}^L - Q_{Xf}^R) \bar{\psi}_f \gamma^\mu \gamma_5 \psi_f \right] Z'_\mu.
\end{aligned} \tag{D.6}$$

Eq. (D.6) is the general neutral current for all $U(1)_X$ models studied in this work. Since we are interested in the regime in which the mixing angle is much smaller than one, $\xi \ll 1$, and $g_X \ll 1$, then Z properties will be kept unmodified.

For concreteness, we shall obtain again the neutral current for a well-known model, such as the $U(1)_{B-L}$ model. In this case, we find

$$\begin{aligned}
\mathcal{L} = & -eJ_{em}^\mu A_\mu - \frac{g_Z}{2} J_{NC}^\mu Z_\mu - \left(\epsilon e J_{em}^\mu + \frac{\epsilon_Z g_Z}{2} J_{NC}^\mu \right) Z'_\mu \\
& - \frac{\epsilon_Z g_Z}{2} \left[\frac{a}{4 \cos^2 \beta} \bar{\psi}_f \gamma^\mu \psi_f \right] Z'_\mu,
\end{aligned} \tag{D.7}$$

Here $a = -2$ for charged leptons and $a = 2/3$ for quarks. Notice that in our case we have a new vector coupling for Z' when compared to the Z' of the Dark 2HDM [41].

E Comparison with the 2HDM with Gauged $U(1)_N$

It is important to cross-check our findings with the existing literature. In [41] a 2HDM similar to the $U(1)_N$ model in Table 2 was studied. Therefore, in this setup all fermions are uncharged under the $U(1)_X$ symmetry, i.e. $Q_X^{L,R} = 0$. Using Eq. (D.5) the neutral current involving the Z boson reads

$$\mathcal{L}_Z = -\frac{g_Z}{2} \cos \xi J_{NC}^\mu Z_\mu - \epsilon g_Z \tan \theta_W \sin \xi \left[\left(\frac{T_{3f}}{2} - Q_f \right) \bar{\psi}_f \gamma^\mu \psi_f - \frac{T_{3f}}{2} \bar{\psi}_f \gamma^\mu \gamma_5 \psi_f \right] Z_\mu. \quad (\text{E.1})$$

Since the mixing angle (ξ) and the kinetic mixing (ϵ) are much smaller than one, only the SM neutral current, the first term of Eq. (E.1) is left. In other words, the Z properties are kept identical to the SM.

As for the neutral current of the Z' boson, we get from Eq. (D.5) that

$$\begin{aligned} \mathcal{L}_{Z'} = & -g_Z \sin \xi \left[\left(\frac{T_{3f}}{2} - Q_f \sin^2 \theta_W \right) \bar{\psi}_f \gamma^\mu \psi_f - \frac{T_{3f}}{2} \bar{\psi}_f \gamma^\mu \gamma_5 \psi_f \right] Z'_\mu \\ & + \epsilon g_Z \tan \theta_W \cos \xi \left[\left(\frac{T_{3f}}{2} - Q_f \right) \bar{\psi}_f \gamma^\mu \psi_f - \frac{1}{2} T_{3f} \bar{\psi}_f \gamma^\mu \gamma_5 \psi_f \right] Z'_\mu. \end{aligned} \quad (\text{E.2})$$

Using Eq. (B.32) and taking $\xi \ll 1$, we find

$$\mathcal{L}_{Z'} = -\epsilon e Q_f \bar{\psi}_f \gamma^\mu \psi_f Z'_\mu - \frac{\epsilon_Z g_Z}{2} [(T_{3f} - 2Q_f \sin^2 \theta_W) \bar{\psi}_f \gamma^\mu \psi_f - T_{3f} \bar{\psi}_f \gamma^\mu \gamma_5 \psi_f] Z'_\mu \quad (\text{E.3})$$

which simplifies to

$$\mathcal{L}_{Z'} = - \left(\epsilon e J_{em}^\mu + \frac{\epsilon_Z g_Z}{2} J_{NC}^\mu \right) Z'_\mu. \quad (\text{E.4})$$

Our limiting case of the $U(1)_N$ model matches the result of [41], once again validating our findings.

F Higgs Interactions to Vector Bosons

In this section we summarize the Higgs-gauge boson vertices under the assumption that the mixing between the Higgs doublets and the singlet scalar is suppressed. We find that

$$\mathcal{C}_{H-Z-Z} = \frac{g_Z^2 v}{2} \cos(\beta - \alpha), \quad (\text{F.1})$$

$$\mathcal{C}_{H-Z-Z'} = -g_Z g_X v \cos \beta \sin \beta \sin(\beta - \alpha), \quad (\text{F.2})$$

$$\mathcal{C}_{H-Z'-Z'} = 2g_X^2 v \cos \beta \sin \beta (\cos^3 \beta \sin \alpha + \sin^3 \beta \cos \alpha), \quad (\text{F.3})$$

$$\mathcal{C}_{h-Z-Z} = \frac{g_Z^2 v}{2} \sin(\beta - \alpha), \quad (\text{F.4})$$

$$\mathcal{C}_{h-Z-Z'} = -g_Z g_X v \cos \beta \sin \beta \cos(\beta - \alpha), \quad (\text{F.5})$$

$$\mathcal{C}_{h-Z'-Z'} = 2g_X^2 v \cos \beta \sin \beta (\cos^3 \beta \sin \alpha - \sin^3 \beta \cos \alpha). \quad (\text{F.6})$$

References

- [1] **ATLAS Collaboration** Collaboration, G. Aad *et. al.*, *Observation of a new particle in the search for the Standard Model Higgs boson with the ATLAS detector at the LHC*, *Phys.Lett.* **B716** (2012) 1–29, [[1207.7214](#)].
- [2] **CMS Collaboration**, S. Chatrchyan *et. al.*, *Observation of a new boson at a mass of 125 GeV with the CMS experiment at the LHC*, *Phys. Lett.* **B716** (2012) 30–61, [[1207.7235](#)].
- [3] S.-Q. Wang, X.-G. Wu, J.-M. Shen, H.-Y. Han, and Y. Ma, *QCD improved electroweak parameter*, *Phys. Rev.* **D89** (2014), no. 11 116001, [[1402.0975](#)].
- [4] G. C. Branco, P. M. Ferreira, L. Lavoura, M. N. Rebelo, M. Sher, and J. P. Silva, *Theory and phenomenology of two-Higgs-doublet models*, *Phys. Rept.* **516** (2012) 1–102, [[1106.0034](#)].
- [5] B. Dasgupta, E. Ma, and K. Tsumura, *Weakly interacting massive particle dark matter and radiative neutrino mass from Peccei-Quinn symmetry*, *Phys. Rev.* **D89** (2014), no. 4 041702, [[1308.4138](#)].
- [6] Y. Mambrini, S. Profumo, and F. S. Queiroz, *Dark Matter and Global Symmetries*, *Phys. Lett.* **B760** (2016) 807–815, [[1508.06635](#)].
- [7] A. Alves, D. A. Camargo, A. G. Dias, R. Longas, C. C. Nishi, and F. S. Queiroz, *Collider and Dark Matter Searches in the Inert Doublet Model from Peccei-Quinn Symmetry*, *JHEP* **10** (2016) 015, [[1606.07086](#)].
- [8] K. Funakubo, A. Kakuto, and K. Takenaga, *The Effective potential of electroweak theory with two massless Higgs doublets at finite temperature*, *Prog. Theor. Phys.* **91** (1994) 341–352, [[hep-ph/9310267](#)].
- [9] A. T. Davies, C. D. Froggatt, G. Jenkins, and R. G. Moorhouse, *Baryogenesis constraints on two Higgs doublet models*, *Phys. Lett.* **B336** (1994) 464–470.
- [10] J. M. Cline, K. Kainulainen, and A. P. Vischer, *Dynamics of two Higgs doublet CP violation and baryogenesis at the electroweak phase transition*, *Phys. Rev.* **D54** (1996) 2451–2472, [[hep-ph/9506284](#)].
- [11] M. Aoki, S. Kanemura, K. Tsumura, and K. Yagyu, *Models of Yukawa interaction in the two Higgs doublet model, and their collider phenomenology*, *Phys. Rev.* **D80** (2009) 015017, [[0902.4665](#)].
- [12] Y. Bai, V. Barger, L. L. Everett, and G. Shaughnessy, *General two Higgs doublet model (2HDM-G) and Large Hadron Collider data*, *Phys. Rev.* **D87** (2013) 115013, [[1210.4922](#)].
- [13] V. Barger, L. L. Everett, H. E. Logan, and G. Shaughnessy, *Scrutinizing the 125 GeV Higgs boson in two Higgs doublet models at the LHC, ILC, and Muon Collider*, *Phys. Rev.* **D88** (2013), no. 11 115003, [[1308.0052](#)].

- [14] B. Dumont, J. F. Gunion, Y. Jiang, and S. Kraml, *Constraints on and future prospects for Two-Higgs-Doublet Models in light of the LHC Higgs signal*, *Phys. Rev.* **D90** (2014) 035021, [[1405.3584](#)].
- [15] H. E. Haber and G. L. Kane, *The search for supersymmetry: probing physics beyond the standard model*, *Phys. Rept.* **117** (1985) 75–263.
- [16] M. Lindner, M. Platscher, and F. S. Queiroz, *A Call for New Physics : The Muon Anomalous Magnetic Moment and Lepton Flavor Violation*, [1610.06587](#).
- [17] S. Davidson, $\mu \rightarrow e\gamma$ in the 2HDM: an exercise in EFT, *Eur. Phys. J.* **C76** (2016), no. 5 258, [[1601.01949](#)].
- [18] M. Misiak and M. Steinhauser, *Weak Radiative Decays of the B Meson and Bounds on M_{H^\pm} in the Two-Higgs-Doublet Model*, [1702.04571](#).
- [19] P. Ko, Y. Omura, and C. Yu, *Higgs phenomenology in Type-I 2HDM with $U(1)_H$ Higgs gauge symmetry*, *JHEP* **01** (2014) 016, [[1309.7156](#)].
- [20] P. Ko, Y. Omura, and C. Yu, *Dark matter and dark force in the type-I inert 2HDM with local $U(1)_H$ gauge symmetry*, *JHEP* **11** (2014) 054, [[1405.2138](#)].
- [21] A. Crivellin, G. D’Ambrosio, and J. Heeck, *Explaining $h \rightarrow \mu^\pm \tau^\mp$, $B \rightarrow K^* \mu^+ \mu^-$ and $B \rightarrow K \mu^+ \mu^- / B \rightarrow K e^+ e^-$ in a two-Higgs-doublet model with gauged $L_\mu - L_\tau$* , *Phys. Rev. Lett.* **114** (2015) 151801, [[1501.00993](#)].
- [22] W.-C. Huang, Y.-L. S. Tsai, and T.-C. Yuan, *G2HDM : Gauged Two Higgs Doublet Model*, *JHEP* **04** (2016) 019, [[1512.00229](#)].
- [23] W. Wang and Z.-L. Han, *Global $U(1)_L$ Breaking in Neutrinophilic 2HDM: From LHC Signatures to X-Ray Line*, *Phys. Rev.* **D94** (2016), no. 5 053015, [[1605.00239](#)].
- [24] **Particle Data Group** Collaboration, C. Patrignani *et. al.*, *Review of Particle Physics*, *Chin. Phys.* **C40** (2016), no. 10 100001.
- [25] T. D. Lee, *A theory of spontaneous t violation*, *Phys. Rev.* **D8** (1973) 1226–1239.
- [26] D. Atwood, L. Reina, and A. Soni, *Phenomenology of two Higgs doublet models with flavor changing neutral currents*, *Phys. Rev.* **D55** (1997) 3156–3176, [[hep-ph/9609279](#)].
- [27] E. A. Paschos, *Diagonal Neutral Currents*, *Phys. Rev.* **D15** (1977) 1966.
- [28] S. L. Glashow and S. Weinberg, *Natural Conservation Laws for Neutral Currents*, *Phys. Rev.* **D15** (1977) 1958.
- [29] P. Ko, Y. Omura, and C. Yu, *A Resolution of the Flavor Problem of Two Higgs Doublet Models with an Extra $U(1)_H$ Symmetry for Higgs Flavor*, *Phys. Lett.* **B717** (2012) 202–206, [[1204.4588](#)].
- [30] A. Alves, S. Profumo, and F. S. Queiroz, *The dark Z' portal: direct, indirect and collider searches*, *JHEP* **04** (2014) 063, [[1312.5281](#)].

- [31] P. Minkowski, *mu -> e gamma at a rate of one out of 1-billion muon decays?*, *Phys. Lett.* **B67** (1977) 421.
- [32] R. N. Mohapatra and G. Senjanovic, *Neutrino Mass and Spontaneous Parity Violation*, *Phys. Rev. Lett.* **44** (1980) 912.
- [33] G. Lazarides, Q. Shafi, and C. Wetterich, *Proton lifetime and fermion masses in an SO(10) model*, *Nucl. Phys.* **B181** (1981) 287.
- [34] R. N. Mohapatra and G. Senjanovic, *Neutrino masses and mixings in gauge models with spontaneous parity violation*, *Phys. Rev.* **D23** (1981) 165.
- [35] J. Schechter and J. Valle, *Neutrino Masses in SU(2) x U(1) Theories*, *Phys.Rev.* **D22** (1980) 2227.
- [36] **Planck** Collaboration, P. A. R. Ade *et. al.*, *Planck 2015 results. XIII. Cosmological parameters*, *Astron. Astrophys.* **594** (2016) A13, [[1502.01589](#)].
- [37] H. Davoudiasl, H.-S. Lee, and W. J. Marciano, *Muon Anomaly and Dark Parity Violation*, *Phys. Rev. Lett.* **109** (2012) 031802, [[1205.2709](#)].
- [38] H. Davoudiasl, H.-S. Lee, and W. J. Marciano, *'Dark' Z implications for Parity Violation, Rare Meson Decays, and Higgs Physics*, *Phys. Rev.* **D85** (2012) 115019, [[1203.2947](#)].
- [39] H. Davoudiasl, H.-S. Lee, I. Lewis, and W. J. Marciano, *Higgs Decays as a Window into the Dark Sector*, *Phys. Rev.* **D88** (2013), no. 1 015022, [[1304.4935](#)].
- [40] H.-S. Lee and E. Ma, *Gauged B - x_iL origin of R Parity and its implications*, *Phys. Lett.* **B688** (2010) 319–322, [[1001.0768](#)].
- [41] H.-S. Lee and M. Sher, *Dark Two Higgs Doublet Model*, *Phys. Rev.* **D87** (2013), no. 11 115009, [[1303.6653](#)].
- [42] H.-S. Lee, *Muon g2 anomaly and dark leptonic gauge boson*, *Phys. Rev.* **D90** (2014), no. 9 091702, [[1408.4256](#)].
- [43] H. Davoudiasl, H.-S. Lee, and W. J. Marciano, *Muon g2, rare kaon decays, and parity violation from dark bosons*, *Phys. Rev.* **D89** (2014), no. 9 095006, [[1402.3620](#)].
- [44] B. Batell, R. Essig, and Z. Surujon, *Strong Constraints on Sub-GeV Dark Sectors from SLAC Beam Dump E137*, *Phys. Rev. Lett.* **113** (2014), no. 17 171802, [[1406.2698](#)].
- [45] W. Rodejohann and C. E. Yaguna, *Scalar dark matter in the BL model*, *JCAP* **1512** (2015), no. 12 032, [[1509.04036](#)].
- [46] K. Kaneta, Z. Kang, and H.-S. Lee, *Right-handed neutrino dark matter under the BL gauge interaction*, *JHEP* **02** (2017) 031, [[1606.09317](#)].
- [47] B. Batell, M. Pospelov, and B. Shuve, *Shedding Light on Neutrino Masses with Dark Forces*, *JHEP* **08** (2016) 052, [[1604.06099](#)].

- [48] A. Alves, G. Arcadi, Y. Mambrini, S. Profumo, and F. S. Queiroz, *Augury of darkness: the low-mass dark Z portal*, *JHEP* **04** (2017) 164, [[1612.07282](#)].
- [49] K. S. Babu, C. F. Kolda, and J. March-Russell, *Implications of generalized Z - Z-prime mixing*, *Phys. Rev.* **D57** (1998) 6788–6792, [[hep-ph/9710441](#)].
- [50] P. Langacker, *The Physics of Heavy Z' Gauge Bosons*, *Rev. Mod. Phys.* **81** (2009) 1199–1228, [[0801.1345](#)].
- [51] S. Gopalakrishna, S. Jung, and J. D. Wells, *Higgs boson decays to four fermions through an abelian hidden sector*, *Phys. Rev.* **D78** (2008) 055002, [[0801.3456](#)].
- [52] M. Klasen, F. Lyonnet, and F. S. Queiroz, *NLO+NLL Collider Bounds, Dirac Fermion and Scalar Dark Matter in the B-L Model*, [1607.06468](#).
- [53] **E865** Collaboration, R. Appel *et. al.*, *A New measurement of the properties of the rare decay $K^+ \rightarrow \pi^+ e^+ e^-$* , *Phys. Rev. Lett.* **83** (1999) 4482–4485, [[hep-ex/9907045](#)].
- [54] **NA48/2** Collaboration, J. R. Batley *et. al.*, *Precise measurement of the $K^+ \rightarrow \pi^+ e^+ e^-$ decay*, *Phys. Lett.* **B677** (2009) 246–254, [[0903.3130](#)].
- [55] L. J. Hall and M. B. Wise, *FLAVOR CHANGING HIGGS - BOSON COUPLINGS*, *Nucl. Phys.* **B187** (1981) 397–408.
- [56] A. J. Buras, *New physics patterns in ϵ'/ϵ and ϵ_K with implications for rare kaon decays and ΔM_K* , *JHEP* **04** (2016) 071, [[1601.00005](#)].
- [57] A. Crivellin, G. D'Ambrosio, M. Hoferichter, and L. C. Tunstall, *Violation of lepton flavor and lepton flavor universality in rare kaon decays*, *Phys. Rev.* **D93** (2016), no. 7 074038, [[1601.00970](#)].
- [58] N. H. Christ, X. Feng, A. Juttner, A. Lawson, A. Portelli, and C. T. Sachrajda, *First exploratory calculation of the long-distance contributions to the rare kaon decays $K \rightarrow \pi \ell^+ \ell^-$* , *Phys. Rev.* **D94** (2016), no. 11 114516, [[1608.07585](#)].
- [59] M. Ibe, W. Nakano, and M. Suzuki, *Constraints on $L_\mu - L_\tau$ Gauge Interactions from Rare Kaon Decay*, [1611.08460](#).
- [60] C.-W. Chiang and P.-Y. Tseng, *Probing a dark photon using rare leptonic kaon and pion decays*, *Phys. Lett.* **B767** (2017) 289–294, [[1612.06985](#)].
- [61] B. Batell, M. Pospelov, and A. Ritz, *Multi-lepton Signatures of a Hidden Sector in Rare B Decays*, *Phys. Rev.* **D83** (2011) 054005, [[0911.4938](#)].
- [62] M. Freytsis, Z. Ligeti, and J. Thaler, *Constraining the Axion Portal with $B \rightarrow K l^+ l^-$* , *Phys. Rev.* **D81** (2010) 034001, [[0911.5355](#)].
- [63] **BaBar** Collaboration, G. Eigen, *Branching Fraction and CP Asymmetry Measurements in Inclusive $B \rightarrow X_s \ell^+ \ell^-$ and $B \rightarrow X_s \gamma$ Decays from BaBar*, *Nucl. Part. Phys. Proc.* **273-275** (2016) 1459–1464, [[1503.02294](#)].
- [64] **BaBar** Collaboration, B. Aubert *et. al.*, *Direct CP, Lepton Flavor and Isospin*

- Asymmetries in the Decays $B \rightarrow K^{(*)}\ell^+\ell^-$* , *Phys. Rev. Lett.* **102** (2009) 091803, [[0807.4119](#)].
- [65] **Belle** Collaboration, J. T. Wei *et. al.*, *Measurement of the Differential Branching Fraction and Forward-Backward Asymmetry for $B \rightarrow K^{(*)}\ell^+\ell^-$* , *Phys. Rev. Lett.* **103** (2009) 171801, [[0904.0770](#)].
- [66] **ALEPH** Collaboration, R. Barate *et. al.*, *Search for an invisibly decaying Higgs boson in e^+e^- collisions at 189-GeV*, *Phys. Lett.* **B466** (1999) 50–60.
- [67] **L3** Collaboration, P. Achard *et. al.*, *Search for an invisibly-decaying Higgs boson at LEP*, *Phys. Lett.* **B609** (2005) 35–48, [[hep-ex/0501033](#)].
- [68] **OPAL** Collaboration, G. Abbiendi *et. al.*, *Search for invisibly decaying Higgs bosons in $e^+e^- \rightarrow Z0 h0$ production at $s^{**}(1/2) = 183\text{-GeV} - 209\text{-GeV}$* , *Phys. Lett.* **B682** (2010) 381–390, [[0707.0373](#)].
- [69] M. Carena, A. de Gouvea, A. Freitas, and M. Schmitt, *Invisible Z boson decays at e^+e^- colliders*, *Phys. Rev.* **D68** (2003) 113007, [[hep-ph/0308053](#)].
- [70] P. M. Ferreira, R. Santos, M. Sher, and J. P. Silva, *Could the LHC two-photon signal correspond to the heavier scalar in two-Higgs-doublet models?*, *Phys. Rev.* **D85** (2012) 035020, [[1201.0019](#)].
- [71] **OPAL, DELPHI, L3, ALEPH, LEP Higgs Working Group for Higgs boson searches** Collaboration, *Search for charged Higgs bosons: Preliminary combined results using LEP data collected at energies up to 209-GeV*, in *Lepton and photon interactions at high energies. Proceedings, 20th International Symposium, LP 2001, Rome, Italy, July 23-28, 2001*, 2001. [hep-ex/0107031](#).
- [72] M. Jung, A. Pich, and P. Tuzon, *Charged-Higgs phenomenology in the Aligned two-Higgs-doublet model*, *JHEP* **11** (2010) 003, [[1006.0470](#)].
- [73] M. Aoki, R. Guedes, S. Kanemura, S. Moretti, R. Santos, and K. Yagyu, *Light Charged Higgs bosons at the LHC in 2HDMs*, *Phys. Rev.* **D84** (2011) 055028, [[1104.3178](#)].
- [74] **ATLAS Collaboration** Collaboration, G. Aad *et. al.*, *Search for charged Higgs bosons decaying via $H^+ \rightarrow \tau\nu$ in top quark pair events using pp collision data at $\sqrt{s} = 7\text{ TeV}$ with the ATLAS detector*, *JHEP* **1206** (2012) 039, [[1204.2760](#)].
- [75] A. Djouadi, J. Kalinowski, and P. M. Zerwas, *Two and three-body decay modes of SUSY Higgs particles*, *Z. Phys.* **C70** (1996) 435–448, [[hep-ph/9511342](#)].
- [76] A. G. Akeroyd, *Three body decays of Higgs bosons at LEP-2 and application to a hidden fermiophobic Higgs*, *Nucl. Phys.* **B544** (1999) 557–575, [[hep-ph/9806337](#)].
- [77] R. Ramos and M. Sher, *The Dark Z and Charged Higgs Decay*, [1312.0013](#).
- [78] C. Bouchiat and P. Fayet, *Constraints on the parity-violating couplings of a new gauge boson*, *Phys. Lett.* **B608** (2005) 87–94, [[hep-ph/0410260](#)].

- [79] W. J. Marciano and A. Sirlin, *RADIATIVE CORRECTIONS TO ATOMIC PARITY VIOLATION*, *Phys. Rev.* **D27** (1983) 552.
- [80] S. G. Porsev, K. Beloy, and A. Derevianko, *Precision determination of weak charge of ^{133}Cs from atomic parity violation*, *Phys. Rev.* **D82** (2010) 036008, [[1006.4193](#)].
- [81] S. C. Bennett and C. E. Wieman, *Measurement of the $6S \rightarrow 7S$ transition polarizability in atomic cesium and an improved test of the Standard Model*, *Phys. Rev. Lett.* **82** (1999) 2484–2487, [[hep-ex/9903022](#)]. [Erratum: *Phys. Rev. Lett.* **83**, 889 (1999)].
- [82] **MOLLER** Collaboration, J. Benesch *et. al.*, *The MOLLER Experiment: An Ultra-Precise Measurement of the Weak Mixing Angle Using Møller Scattering*, [1411.4088](#).
- [83] N. Berger *et. al.*, *Measuring the weak mixing angle with the P2 experiment at MESA*, *J. Univ. Sci. Tech. China* **46** (2016), no. 6 481–487, [[1511.03934](#)].
- [84] R. Bucoveanu, M. Gorchtein, and H. Spiesberger, *Precision Measurement of $\sin^2 \theta_w$ at MESA*, *PoS LL2016* (2016) 061, [[1606.09268](#)].
- [85] R. L. Garwin, D. P. Hutchinson, S. Penman, and G. Shapiro, *Accurate Determination of the μ^+ Magnetic Moment*, *Phys. Rev.* **118** (1960) 271–283.
- [86] T. Burnett and M. J. Levine, *Intermediate vector boson contribution to the muon’s anomalous magnetic moment*, *Phys. Lett.* **B24** (1967) 467–468.
- [87] T. Kinoshita and R. J. Oakes, *Hadronic contributions to the muon magnetic moment*, *Phys. Lett.* **25B** (1967) 143–145.
- [88] T. Blum, A. Denig, I. Logashenko, E. de Rafael, B. Lee Roberts, T. Teubner, and G. Venanzoni, *The Muon ($g-2$) Theory Value: Present and Future*, [1311.2198](#).
- [89] J. P. Leveille, *The Second Order Weak Correction to ($G-2$) of the Muon in Arbitrary Gauge Models*, *Nucl. Phys.* **B137** (1978) 63–76.
- [90] F. Jegerlehner and A. Nyffeler, *The Muon $g-2$* , *Phys. Rept.* **477** (2009) 1–110, [[0902.3360](#)].
- [91] F. S. Queiroz and W. Shepherd, *New Physics Contributions to the Muon Anomalous Magnetic Moment: A Numerical Code*, *Phys. Rev.* **D89** (2014), no. 9 095024, [[1403.2309](#)].
- [92] S. Profumo and F. S. Queiroz, *Constraining the Z' mass in 331 models using direct dark matter detection*, *Eur. Phys. J.* **C74** (2014), no. 7 2960, [[1307.7802](#)].
- [93] B. Allanach, F. S. Queiroz, A. Strumia, and S. Sun, *Z models for the LHCb and $g - 2$ muon anomalies*, *Phys. Rev.* **D93** (2016), no. 5 055045, [[1511.07447](#)].
- [94] A. Alves, A. Berlin, S. Profumo, and F. S. Queiroz, *Dirac-fermionic dark matter in $U(1)_X$ models*, *JHEP* **10** (2015) 076, [[1506.06767](#)].
- [95] A. Alves, A. Berlin, S. Profumo, and F. S. Queiroz, *Dark Matter Complementarity and the Z' Portal*, *Phys. Rev.* **D92** (2015), no. 8 083004, [[1501.03490](#)].

- [96] S. Patra, F. S. Queiroz, and W. Rodejohann, *Stringent Dilepton Bounds on Left-Right Models using LHC data*, *Phys. Lett.* **B752** (2016) 186–190, [[1506.03456](#)].
- [97] CMS Collaboration, V. Khachatryan *et. al.*, *Search for narrow resonances in dilepton mass spectra in proton-proton collisions at $\sqrt{s} = 13$ TeV and combination with 8 TeV data*, *Phys. Lett.* **B768** (2017) 57–80, [[1609.05391](#)].
- [98] M. Lindner, F. S. Queiroz, and W. Rodejohann, *Dilepton bounds on leftright symmetry at the LHC run II and neutrinoless double beta decay*, *Phys. Lett.* **B762** (2016) 190–195, [[1604.07419](#)].
- [99] W. Altmannshofer, S. Gori, S. Profumo, and F. S. Queiroz, *Explaining dark matter and B decay anomalies with an $L_\mu - L_\tau$ model*, *JHEP* **12** (2016) 106, [[1609.04026](#)].
- [100] ATLAS Collaboration, T. A. collaboration, *Search for new high-mass phenomena in the dilepton final state using 36.1 fb^{-1} of proton-proton collision data at $\sqrt{s} = 13$ TeV with the ATLAS detector*, .
- [101] G. Arcadi, M. Dutra, P. Ghosh, M. Lindner, Y. Mambrini, M. Pierre, S. Profumo, and F. S. Queiroz, *The Waning of the WIMP? A Review of Models, Searches, and Constraints*, [1703.07364](#).
- [102] O. G. Miranda, V. B. Semikoz, and J. W. F. Valle, *Neutrino electron scattering and electroweak gauge structure: Probing the masses of a new Z boson*, in *Lepton and baryon number violation in particle physics, astrophysics and cosmology. Proceedings, 1st International Symposium, Lepton-baryon'98, Trento, Italy, April 20-25, 1998*, pp. 683–690, 1998. [hep-ph/9808395](#).
- [103] S. Ciechanowicz, W. Sobkow, and M. Misiaszek, *Scattering of neutrinos on a polarized electron target as a test for new physics beyond the standard model*, *Phys. Rev.* **D71** (2005) 093006, [[hep-ph/0309286](#)].
- [104] J. Kopp, P. A. N. Machado, and S. J. Parke, *Interpretation of MINOS data in terms of non-standard neutrino interactions*, *Phys. Rev.* **D82** (2010) 113002, [[1009.0014](#)].
- [105] R. Harnik, J. Kopp, and P. A. N. Machado, *Exploring ν Signals in Dark Matter Detectors*, *JCAP* **1207** (2012) 026, [[1202.6073](#)].
- [106] W. Liao, X.-H. Wu, and H. Zhou, *Electron events from the scattering with solar neutrinos in the search of keV scale sterile neutrino dark matter*, *Phys. Rev.* **D89** (2014), no. 9 093017, [[1311.6075](#)].
- [107] W. Rodejohann, X.-J. Xu, and C. E. Yaguna, *Distinguishing between Dirac and Majorana neutrinos in the presence of general interactions*, *JHEP* **05** (2017) 024, [[1702.05721](#)].
- [108] S. Bilmis, I. Turan, T. M. Aliev, M. Deniz, L. Singh, and H. T. Wong, *Constraints on Dark Photon from Neutrino-Electron Scattering Experiments*, *Phys. Rev.* **D92** (2015), no. 3 033009, [[1502.07763](#)].

- [109] J. Alexander *et. al.*, *Dark Sectors 2016 Workshop: Community Report*, 2016. [1608.08632](#).
- [110] J.-W. Chen, H.-C. Chi, H.-B. Li, C. P. Liu, L. Singh, H. T. Wong, C.-L. Wu, and C.-P. Wu, *Constraints on millicharged neutrinos via analysis of data from atomic ionizations with germanium detectors at sub-keV sensitivities*, *Phys. Rev.* **D90** (2014), no. 1 011301, [[1405.7168](#)].
- [111] **TEXONO collaboration** Collaboration, H. B. Li *et. al.*, *New limits on neutrino magnetic moments from the kuo-sheng reactor neutrino experiment*, [hep-ex/0212003](#).
- [112] **TEXONO** Collaboration, H. T. Wong *et. al.*, *A Search of Neutrino Magnetic Moments with a High-Purity Germanium Detector at the Kuo-Sheng Nuclear Power Station*, *Phys. Rev.* **D75** (2007) 012001, [[hep-ex/0605006](#)].
- [113] **TEXONO collaboration** Collaboration, M. Deniz *et. al.*, *Measurement of Neutrino-Electron Scattering Cross-Section with a CsI(Tl) Scintillating Crystal Array at the Kuo-Sheng Nuclear Power Reactor*, *Phys. Rev.* **D81** (2010) 072001, [[0911.1597](#)].
- [114] **LSND collaboration** Collaboration, L. B. Auerbach *et. al.*, *Measurement of electron-neutrino electron elastic scattering*, *Phys. Rev.* **D63** (2001) 112001, [[hep-ex/0101039](#)].
- [115] G. Bellini, J. Benziger, D. Bick, S. Bonetti, G. Bonfini, *et. al.*, *Precision measurement of the ^7Be solar neutrino interaction rate in Borexino*, *Phys.Rev.Lett.* **107** (2011) 141302, [[1104.1816](#)].
- [116] A. G. Beda, E. V. Demidova, A. S. Starostin, V. B. Brudanin, V. G. Egorov, D. V. Medvedev, M. V. Shirchenko, and T. Vylov, *GEMMA experiment: Three years of the search for the neutrino magnetic moment*, *Phys. Part. Nucl. Lett.* **7** (2010) 406–409, [[0906.1926](#)].
- [117] **CHARM-II** Collaboration, P. Vilain *et. al.*, *Measurement of differential cross-sections for muon-neutrino electron scattering*, *Phys. Lett.* **B302** (1993) 351–355.
- [118] M. Pospelov, A. Ritz, and M. B. Voloshin, *Secluded WIMP Dark Matter*, *Phys. Lett.* **B662** (2008) 53–61, [[0711.4866](#)].
- [119] M. Pospelov, *Secluded $U(1)$ below the weak scale*, *Phys. Rev.* **D80** (2009) 095002, [[0811.1030](#)].
- [120] G. Arcadi, Y. Mambrini, M. H. G. Tytgat, and B. Zaldivar, *Invisible Z' and dark matter: LHC vs LUX constraints*, *JHEP* **03** (2014) 134, [[1401.0221](#)].
- [121] G. Arcadi, Y. Mambrini, and F. Richard, *Z-portal dark matter*, *JCAP* **1503** (2015) 018, [[1411.2985](#)].
- [122] G. Arcadi, Y. Mambrini, and M. Pierre, *Impact of Dark Matter Direct and Indirect*

- Detection on Simplified Dark Matter Models*, *PoS EPS-HEP2015* (2015) 396, [[1510.02297](#)].
- [123] G. Arcadi, C. Gross, O. Lebedev, S. Pokorski, and T. Toma, *Evading Direct Dark Matter Detection in Higgs Portal Models*, *Phys. Lett.* **B769** (2017) 129–133, [[1611.09675](#)].
- [124] G. Arcadi, C. Gross, O. Lebedev, Y. Mambrini, S. Pokorski, and T. Toma, *Multicomponent Dark Matter from Gauge Symmetry*, *JHEP* **12** (2016) 081, [[1611.00365](#)].